

# Successful Leptogenesis in $SO(10)$ Unification with a Left-Right Symmetric Seesaw Mechanism

Asmaa Abada<sup>a</sup>, Pierre Hosteins<sup>b</sup>, François-Xavier Josse-Michaux<sup>a</sup>  
and Stéphane Lavignac<sup>c</sup>

<sup>a</sup> *Laboratoire de Physique Théorique, UMR 8627, Université de Paris-Sud 11, Bâtiment 210,  
91405 Orsay Cedex, France*

<sup>b</sup> *Department of Physics, University of Patras, GR-26500 Patras, Greece*

<sup>c</sup> *Institut de Physique Théorique<sup>1</sup>, CEA-Saclay, F-91191 Gif-sur-Yvette Cedex, France*

## Abstract

We study thermal leptogenesis in a broad class of supersymmetric  $SO(10)$  models with a left-right symmetric seesaw mechanism, taking into account flavour effects and the contribution of the next-to-lightest right-handed neutrino supermultiplet. Assuming  $M_D = M_u$  and a normal hierarchy of light neutrino masses, we show that four out of the eight right-handed neutrino mass spectra reconstructed from low-energy neutrino data can lead to successful leptogenesis with a reheating temperature in the  $(10^9 - 10^{10})$  GeV range. In the remaining four solutions, leptogenesis is dominated by  $N_2$  decays, as in the type I seesaw case. We find that some of these spectra can generate the observed baryon asymmetry for reheating temperatures above  $10^{10}$  GeV, in contrast to the type I case. Together with flavour effects, an accurate description of charged fermion masses turns out to be a crucial ingredient in the analysis.

---

<sup>1</sup>Laboratoire de la Direction des Sciences de la Matière du Commissariat à l'Énergie Atomique et Unité de Recherche associée au CNRS (URA 2306).

# 1 Introduction

Leptogenesis is one of the most popular mechanism for generating the observed [1] baryon asymmetry of the universe:

$$\frac{n_B - n_{\bar{B}}}{n_\gamma} = (6.21 \pm 0.16) \times 10^{-10} . \quad (1)$$

In its simplest version [2], out-of-equilibrium decays of heavy Majorana neutrinos generate a lepton asymmetry which is then partially converted into a baryon asymmetry by sphaleron processes [3, 4]. This mechanism has been extensively studied in the last decade [5]. In particular, conditions for a successful leptogenesis have been obtained [6, 7, 8] and many refinements have been added, such as spectator processes [9], finite temperature corrections [8] and flavour effects [10]. One of these conditions is the famous Davidson-Ibarra bound [6] on the lightest right-handed neutrino mass,  $M_1 \geq \mathcal{O}(10^8 - 10^9)$  GeV, which applies in the case of a hierarchical right-handed neutrino mass spectrum. The main outcome of these studies is that thermal leptogenesis can work with parameters consistent with the type I seesaw [11] interpretation of neutrino oscillation data. By contrast, standard electroweak baryogenesis [12] fails to produce the observed baryon asymmetry [13, 14], and its supersymmetric version [15] is successful only in a small portion of the Minimal Supersymmetric Standard Model (MSSM) parameter space<sup>2</sup>.

While thermal leptogenesis can successfully generate the baryon asymmetry of the universe if we are free to choose the right-handed neutrino masses and couplings (modulo the constraints coming from neutrino masses and mixing), this might not be the case if the seesaw mechanism is embedded into a more fundamental theory – typically a Grand Unified Theory (GUT) based on the  $SO(10)$  gauge group [17]. In such theories, the right-handed neutrino parameters are constrained both by the unified gauge symmetry, which implies relations among quark and lepton mass matrices, and by neutrino oscillation data, with no guarantee that they fall into the range preferred by leptogenesis. It is well known indeed [18] that the  $SO(10)$  mass formula  $M_D = M_u$  leads to a strongly hierarchical heavy neutrino mass spectrum (except for special values of the light neutrino parameters [19]), with  $M_1$  lying below the Davidson-Ibarra bound. This conclusion can be evaded, however, if the relation  $M_D = M_u$  receives large corrections from Yukawa couplings involving a  $\mathbf{126}$  or a  $\mathbf{120}$  Higgs representation, as in the so-called minimal  $SO(10)$  model [20] and its extensions, or from non-renormalizable interactions [21]. The contribution of the next-to-lightest right-handed neutrino to the baryon asymmetry could also, in principle, change the above picture [22, 23].

In this paper, we investigate another possibility to reconcile  $SO(10)$  unification with leptogenesis, based on the left-right symmetric seesaw mechanism<sup>3</sup>. In a broad class of  $SO(10)$  models, neutrino masses receive contributions from both the type I [11] (right-handed neutrino exchange) and the type II [27] (heavy scalar  $SU(2)_L$  triplet exchange) seesaw mechanisms, with both contributions related by a left-right symmetry. As a result, for a given Dirac mass matrix, 8 different right-handed neutrino mass spectra are consistent with the same light neutrino mass matrix [28], instead of a single one in the type I case. It was shown in Ref. [29] (albeit with a qualitative discussion of the washout) that some of these spectra can lead to successful leptogenesis even if the mass relation  $M_D = M_u$  holds. This was confirmed, for the case of an inverted light neutrino mass hierarchy, in Ref. [30], where the Boltzmann equations were solved in the one-flavour approximation (the possibility of triplet leptogenesis has also been studied in Ref. [31]). The purpose of the present paper is to perform a more comprehensive study of thermal leptogenesis in this class of  $SO(10)$  models, including previously missing ingredients such as flavour effects and the contribution of the next-to-lightest right-handed neutrino, and investigating the dependence of the final baryon asymmetry on low- and high-energy parameters as well as on the reheating temperature. The necessary corrections to the GUT-scale mass relation  $M_d = M_e$  are also

---

<sup>2</sup>Electroweak baryogenesis could however still be a viable mechanism in other extensions of the Standard Model in which the dynamics of the electroweak phase transition is modified (see e.g. Ref. [16] for a review).

<sup>3</sup>A completely different option, based on a non-standard embedding of the Standard Model matter fields into  $SO(10)$  representations, has been explored in Refs. [24, 25]. Successful leptogenesis can also be achieved by adding chiral singlets to supersymmetric  $SO(10)$  models [26].

taken into account in our analysis. Assuming  $M_D = M_u$  and a normal hierarchy of light neutrino masses, we find that successful leptogenesis is possible with a reheating temperature in the  $(10^9 - 10^{10})$  GeV range for 4 out of the 8 reconstructed right-handed neutrino spectra. Some of the remaining 4 spectra can also generate the observed baryon asymmetry, but for higher reheating temperatures.

The paper is organized as follows. In Section 2, we review the left-right symmetric seesaw mechanism in supersymmetric  $SO(10)$  models, as well as the properties of the associated right-handed neutrino mass spectra. In Section 3, we write the flavour-dependent Boltzmann equations governing leptogenesis, including the contribution of the next-to-lightest right-handed neutrino and of its supersymmetric partner. In Section 4, we solve numerically the Boltzmann equations and present our results for the final baryon asymmetry, taking into account the corrections to the mass relation  $M_d = M_e$ . In Section 5, we study the dependence of the final baryon asymmetry on the yet unmeasured light neutrino parameters, on the high-energy Dirac couplings and on the reheating temperature. Finally, we present our conclusions in Section 6.

## 2 The framework

### 2.1 The left-right symmetric seesaw mechanism in supersymmetric $SO(10)$ models

One of the appealing features of  $SO(10)$  unification is that it provides a natural realization of the seesaw mechanism, thus yielding an elegant explanation for the smallness of neutrino masses. Indeed, the right-handed neutrinos needed for the (type I) seesaw mechanism belong to the  $\mathbf{16}_i$  representations ( $i = 1, 2, 3$ ) that contain the Standard Model matter fields, and they acquire heavy Majorana masses at the scale where the  $B - L$  symmetry (which is part of the  $SO(10)$  gauge symmetry) is broken. Namely, the Majorana mass matrix is generated either by the renormalizable operators  $\mathbf{16}_i \mathbf{16}_j \overline{\mathbf{126}}$  or by the non-renormalizable operators  $\mathbf{16}_i \mathbf{16}_j \overline{\mathbf{16}} \overline{\mathbf{16}} / \Lambda$ , in which the  $SU(5)$ -singlet component of the  $\overline{\mathbf{126}}$  (resp.  $\overline{\mathbf{16}}$ ) Higgs representation provides the  $(B - L)$ -breaking vev. As for the Dirac neutrino mass matrix, it arises from the same  $SO(10)$  operators that contribute to the charged fermion masses. Upon integrating out the heavy Majorana neutrinos, one obtains the well-known type I seesaw mass formula:

$$M_\nu^{(I)} = -M_D^T M_R^{-1} M_D, \quad (2)$$

where  $M_D$  and  $M_R$  denote the Dirac and Majorana mass matrices, respectively. In supersymmetric  $SO(10)$  models with a  $\overline{\mathbf{126}}$  Higgs representation, the light neutrino mass matrix can receive an additional type II contribution if a  $\mathbf{54}$  Higgs representation is also present. The role of the  $\mathbf{54}$  is to induce a coupling between the  $\overline{\mathbf{126}}$  representation, in which the  $SU(2)_L$  triplet needed for the type II seesaw mechanism lies, and a  $\mathbf{10}$  representation containing a significant  $H_u$  component<sup>4</sup>, where  $H_u$  is the MSSM Higgs doublet responsible for up quark masses. To see how this works, it is convenient to use a left-right symmetric language: the  $\overline{\mathbf{126}}$  contains a right-handed triplet  $\Delta^c$  with quantum numbers  $(\mathbf{1}, \mathbf{1}, \mathbf{3})_{-2}$  under  $SU(3)_C \times SU(2)_L \times SU(2)_R \times U(1)_{B-L}$ , whose vev  $v_R$  is responsible for the breaking of the  $B - L$  symmetry, as well as a left-handed triplet  $\Delta = (\mathbf{1}, \mathbf{3}, \mathbf{1})_{+2}$ ; the  $\mathbf{54}$  contains a bitriplet  $\tilde{\Delta} = (\mathbf{1}, \mathbf{3}, \mathbf{3})_0$ ; and the  $\mathbf{10}$  contains a bidoublet  $\Phi = (\mathbf{1}, \mathbf{2}, \mathbf{2})_0$ . The superpotential terms relevant for the type II seesaw mechanism read:

$$\frac{1}{2} f_{ij} L_i L_j \Delta + \frac{1}{2} \sigma \Phi \Phi \tilde{\Delta} + \tau \Delta \Delta^c \tilde{\Delta}, \quad (3)$$

where the first term comes from the  $\mathbf{16}_i \mathbf{16}_j \overline{\mathbf{126}}$  couplings, while the second and third terms come from the  $\mathbf{10} \mathbf{10} \mathbf{54}$  and  $\mathbf{54} \overline{\mathbf{126}} \overline{\mathbf{126}}$  couplings, respectively. Setting  $\langle (\Delta^c)^0 \rangle = v_R$  in Eq. (3) and integrating out the heavy triplets  $\Delta$  and  $\tilde{\Delta}$ , one obtains:

$$M_\nu^{(II)} = \frac{\sigma_u v_u^2}{2M_\Delta} f, \quad (4)$$

---

<sup>4</sup>In general,  $H_u$  is a linear combination of all  $Y = +1$   $SU(2)_L$  doublets contained in the Higgs representations of the model. Denoting by  $H_u^{10}$  the  $Y = +1$  doublet lying in the  $\mathbf{10}$  under consideration, one can write  $H_u^{10} = \alpha_u H_u + \dots$ , where the dots stand for heavy  $Y = +1$  doublets. We assume here that  $\alpha_u \sim 1$ , although strictly speaking only  $\alpha_u \neq 0$  is required.

where  $\sigma_u \equiv \alpha_u^2 \sigma$ ,  $v_u \equiv \langle H_u^0 \rangle = v \sin \beta$  ( $v = 174$  GeV), and  $M_\Delta$  is an effective  $SU(2)_L$  triplet mass. The couplings of Eq. (3) alone would give  $M_\Delta = \tau v_R$ , but the superpotential generally contains additional terms contributing to the  $SU(2)_L$  triplet mass matrix. Depending on these,  $M_\Delta$  may be larger or smaller than  $v_R$  (for  $v_R \ll M_{GUT}$ , a tuning of the superpotential parameters is generally necessary to achieve  $M_\Delta < v_R$  [32]). Notice that, due to the left-right symmetry embedded in the  $SO(10)$  gauge symmetry, the same set of parameters  $f_{ij}$  determine the triplet couplings in Eq. (3) and the right-handed neutrino mass matrix, which is given by  $M_R = f v_R$ . Assuming further that the Dirac neutrino mass matrix is symmetric (which excludes a contribution from Yukawa couplings involving a **120** Higgs representation), one ends up with the left-right symmetric seesaw mass formula:

$$M_\nu = \frac{\sigma_u v_u^2}{2M_\Delta} f - \frac{v_u^2}{v_R} Y_\nu f^{-1} Y_\nu, \quad (5)$$

where we have written the Dirac mass matrix as  $M_D \equiv Y_\nu v_u$ .

Definite predictions for the baryon asymmetry generated via leptogenesis require the knowledge of the masses and couplings of the heavy decaying states. In this respect,  $SO(10)$  models provide a predictive framework, since the Dirac mass matrix is generated by the same Yukawa couplings as the charged fermion mass matrices. In the type I seesaw case, one can reconstruct the right-handed neutrino mass matrix  $M_R$  from the knowledge of the light neutrino mass matrix by simply inverting Eq. (2), provided that the Dirac mass matrix is known. Assuming e.g. that  $M_D$  and  $M_u$  only receive contribution from renormalizable Yukawa couplings to 10-dimensional Higgs multiplets, which implies the well-known mass relation  $M_D = M_u$ , one generically obtains a strongly hierarchical right-handed neutrino mass spectrum, with  $M_1$  lying below the Davidson-Ibarra bound [6] (see however Ref. [19] for special situations where  $M_1$  and  $M_2$  can be degenerate). More generally, successful leptogenesis is difficult to achieve in  $SO(10)$  models with a type I seesaw mechanism, even taking into account the contribution of the next-to-lightest right-handed neutrino [29] as suggested in Ref. [23].

In the left-right symmetric seesaw case, the reconstruction of the matrix  $f$  that determines both the right-handed neutrino mass matrix and the triplet couplings requires the resolution of the non-linear matrix equation (5). In Ref. [28], Akhmedov and Frigerio showed that this equation has exactly  $2^n$  solutions in the  $n$  generation case, and provided explicit solutions up to  $n = 3$ . An alternative reconstruction procedure, which employs complex orthogonal matrices, was proposed in Ref. [29]. There it was argued, based on a qualitative discussion of the washout, that this multiplicity of solutions makes it possible for leptogenesis to be successful in  $SO(10)$  models with a left-right symmetric seesaw mechanism. The purpose of the present paper is to put this statement on a quantitative basis, and to prove in particular that successful leptogenesis is indeed possible for “mixed” solutions in which neither the type I nor the type II seesaw contribution dominates in the light neutrino mass matrix.

## 2.2 Reconstruction procedure

Before presenting our study, let us briefly recall the reconstruction procedure of Ref. [29]. Our starting point is the left-right symmetric seesaw formula (5), in which both  $f$  and  $Y_\nu$  are complex symmetric matrices. We want to reconstruct  $f$  for a given pattern of light neutrino masses and lepton mixing, assuming that  $Y_\nu$  is known in a basis in which the charged lepton mass matrix is diagonal. For concreteness, we work in the 3-family case, but the procedure applies to any number of neutrino families.

In order to solve Eq. (5), we first rewrite it as

$$Z = \alpha X - \beta X^{-1}, \quad (6)$$

with  $\alpha \equiv \sigma_u v_u^2 / (2M_\Delta)$ ,  $\beta \equiv v_u^2 / v_R$  and

$$Z \equiv N_\nu^{-1} M_\nu (N_\nu^{-1})^T, \quad X \equiv N_\nu^{-1} f (N_\nu^{-1})^T, \quad (7)$$

where  $N_\nu$  is a matrix such that  $Y_\nu = N_\nu N_\nu^T$ , and  $Y_\nu$  is assumed to be invertible. Being complex and symmetric,  $Z$  can be diagonalized by a complex orthogonal matrix if its eigenvalues (i.e. the roots of the characteristic polynomial  $\det(Z - z\mathbf{1}) = 0$ ) are all distinct:

$$Z = O_Z \text{Diag}(z_1, z_2, z_3) O_Z^T, \quad |z_1| < |z_2| < |z_3|, \quad O_Z O_Z^T = \mathbf{1}. \quad (8)$$

Then Eq. (6) can be solved for  $X$  in a straightforward manner, by noting that  $X$  is diagonalized by the same complex orthogonal matrix as  $Z$ . Upon an  $O_Z$  transformation, Eq. (6) reduces to 3 independent quadratic equations for the eigenvalues of  $X$ :

$$z_i = \alpha x_i - \beta x_i^{-1}. \quad (9)$$

For a given choice of  $(x_1, x_2, x_3)$ , the solution of Eq. (5) is given by:

$$f = N_\nu O_Z \text{Diag}(x_1, x_2, x_3) O_Z^T N_\nu^T. \quad (10)$$

The right-handed neutrino masses  $M_i = f_i v_R$  are obtained by diagonalizing  $f$  with a unitary matrix:

$$f = U_f \text{Diag}(f_1, f_2, f_3) U_f^T, \quad f_1 < f_2 < f_3, \quad U_f U_f^\dagger = \mathbf{1}, \quad (11)$$

where the  $f_i$  are chosen to be real and positive. The matrix  $U_f$  relates the original basis for right-handed neutrinos, in which  $Y_\nu$  is symmetric, to their mass eigenstate basis. It can be used to express the Dirac couplings in terms of charged lepton and right-handed neutrino mass eigenstates, as  $\lambda \equiv U_f^\dagger Y_\nu$ .

Since each equation  $z_i = \alpha x_i - \beta x_i^{-1}$  has two solutions  $x_i^-$  and  $x_i^+$ , there are  $2^3 = 8$  different solutions for the matrix  $f$ , which we label in the following way:  $(+, +, +)$  refers to the solution  $(x_1^+, x_2^+, x_3^+)$ ,  $(+, +, -)$  to the solution  $(x_1^+, x_2^+, x_3^-)$ , and so on. It is convenient to define  $x_i^-$  and  $x_i^+$  such that, in the  $4\alpha\beta \ll |z_i|^2$  limit:

$$x_i^- \simeq -\frac{\beta}{z_i}, \quad x_i^+ \simeq \frac{z_i}{\alpha}. \quad (12)$$

We will refer to  $x_i^-$  as the ‘‘type I branch’’ and to  $x_i^+$  as the ‘‘type II branch’’. This terminology is motivated by the fact that solutions  $(-, -, -)$  and  $(+, +, +)$  reduce to the ‘‘pure’’ type I and type II cases in the large  $v_R$  limit (defined by  $4\alpha\beta \ll |z_1|^2$ , or equivalently  $v_R \gg 2\sigma_u v_u^4 / M_\Delta |z_1|^2$ ):

$$f^{(-,-,-)} \xrightarrow{4\alpha\beta \ll |z_1|^2} -\frac{v_u^2}{v_R} Y_\nu M_\nu^{-1} Y_\nu, \quad (13)$$

$$f^{(+,+,+)} \xrightarrow{4\alpha\beta \ll |z_1|^2} \frac{M_\nu}{\alpha}. \quad (14)$$

The remaining 6 solutions correspond to mixed cases where the light neutrino mass matrix receives significant contributions from both types of seesaw mechanisms. In the opposite, small  $v_R$  limit ( $|z_3|^2 \ll 4\alpha\beta$ ), one has  $x_i^\pm \simeq \pm \text{sign}(\text{Re}(z_i)) \sqrt{\beta/\alpha}$ , which indicates a partial cancellation between the type I and type II contributions to light neutrino masses. Finally, in the region of intermediate  $v_R$  values,  $|z_1|^2 < 4\alpha\beta < |z_3|^2$ , both the type I and the type II seesaw mechanisms give significant contributions to the light neutrino mass matrix.

### 2.3 Properties of the reconstructed right-handed neutrino spectra

The above procedure can be used to determine the a priori unknown  $f_{ij}$  couplings in theories which predict the Dirac matrix  $Y_\nu$ , taking low-energy neutrino data as an input. In Ref. [29], it was applied to supersymmetric  $SO(10)$  models with two  $\mathbf{10}$ 's, a  $\mathbf{54}$  and a pair of  $\mathbf{126} \oplus \overline{\mathbf{126}}$  representations in the Higgs sector, but no  $\mathbf{120}$  representation (as required by the left-right symmetric seesaw mechanism). In this subsection, we recall the main properties of the reconstructed right-handed neutrino mass spectra.

Given the above assumptions, the most general renormalizable Yukawa couplings read:

$$Y_{ij}^{(1)} \mathbf{16}_i \mathbf{16}_j \mathbf{10}_1 + Y_{ij}^{(2)} \mathbf{16}_i \mathbf{16}_j \mathbf{10}_2 + f_{ij} \mathbf{16}_i \mathbf{16}_j \overline{\mathbf{126}}, \quad (15)$$

where  $Y^{(1)}$ ,  $Y^{(2)}$  and  $f$  are complex symmetric matrices. Assuming that the  $SU(2)_L$  doublet components of the  $\overline{\mathbf{126}}$  do not acquire a vev, Eq. (15) leads to the following GUT-scale mass relations:

$$M_u = M_D, \quad M_d = M_e. \quad (16)$$

It is well known that the second relation is in conflict with experimental data and needs to be corrected. In the absence of a  $\mathbf{210}$  Higgs representation that would induce vev's for the doublet components of the  $\overline{\mathbf{126}}$  [33], this must be done by non-renormalizable interactions. We postpone the discussion of this issue to Section 4, and assume for the time being that Eq. (16) holds.

The inputs in the reconstruction procedure are the matrices  $Y_\nu$  and  $M_\nu$  at the seesaw scale. Neglecting the running of  $Y_\nu$  between the GUT scale and the seesaw scale, Eq. (16) yields, in the basis for the  $\mathbf{16}$  matter representations in which  $M_e$  is diagonal with real positive entries:

$$Y_\nu = U_q^T \hat{Y}_u U_q, \quad U_q = P_u V_{CKM} P_d, \quad \hat{Y}_u = \text{Diag}(y_u, y_c, y_t), \quad (17)$$

where  $V_{CKM}$  is the CKM matrix and  $y_{u,c,t}$  are the up quark Yukawa couplings, all renormalized at the GUT scale. The presence of two diagonal matrices of phases  $P_u$  and  $P_d$  in Eq. (17) is due to the fact that the  $SO(10)$  symmetry prevents independent rephasing of right-handed and left-handed quark fields. In the same basis, the light neutrino mass matrix generated from the seesaw mechanism reads:

$$M_\nu = U_l^* \hat{M}_\nu U_l^\dagger, \quad U_l = P_e V_{PMNS} P_\nu, \quad \hat{M}_\nu = \text{Diag}(m_1, m_2, m_3), \quad (18)$$

where  $V_{PMNS}$  contains a single, Dirac-type phase  $\delta_{PMNS}$ , and  $P_e$  and  $P_\nu$  are two diagonal matrices of phases. With the convention that  $P_\nu$  contains only two phases,  $U_{PMNS} \equiv V_{PMNS} P_\nu$  is the PMNS lepton mixing matrix and  $m_{1,2,3}$  are the light neutrino masses, all renormalized at the seesaw scale<sup>5</sup>. The two phases in  $P_\nu$  are the physical CP-violating phases associated with the Majorana nature of the light neutrinos, while the three phases contained in  $P_e$ , analogous to the five independent phases contained in  $P_u$  and  $P_d$ , are pure high-energy phases. Once the input values for  $(y_u, y_c, y_t)$ ,  $(m_1, m_2, m_3)$ ,  $V_{CKM}$  and  $U_{PMNS}$  at the GUT scale are fixed, the 8 different  $f$  matrices can be reconstructed as a function of  $\alpha$ ,  $\beta$  (or, equivalently, of the  $B-L$  breaking scale  $v_R$  and  $\beta/\alpha$ ) and of the high-energy phases contained in  $P_u$ ,  $P_d$  and  $P_e$ . Notice that, as long as Eq. (16) holds, the reconstructed  $f_{ij}$  couplings depend on the combination of phases  $P_d P_e$  rather than on  $P_d$  and  $P_e$  separately; hence the number of independent high-energy phases reduces to five.

Let us specify the input values that we are going to use in this paper. For the quark masses and the CKM parameters at the  $M_Z$  scale, we take the central values given in Refs. [34] and [35], respectively:

$$m_u(M_Z) = 1.7 \text{ MeV}, \quad m_c(M_Z) = 0.62 \text{ GeV}, \quad m_t(M_Z) = 171 \text{ GeV}, \quad (19)$$

$$m_d(M_Z) = 3.0 \text{ MeV}, \quad m_s(M_Z) = 54 \text{ MeV}, \quad m_b(M_Z) = 2.87 \text{ GeV}, \quad (20)$$

$$A(M_Z) = 0.818, \quad \lambda = 0.2272, \quad \bar{\rho} = 0.221, \quad \bar{\sigma} = 0.340. \quad (21)$$

These values, together with the inputs for the lepton mass and mixing parameters, are subsequently evolved to the GUT scale  $M_{GUT} \simeq 2 \times 10^{16}$  GeV using the Mathematica package REAP [36] with an effective supersymmetric threshold  $M_{SUSY} = 1$  TeV and  $\tan \beta = 10$ . Our reference light neutrino spectrum is a normal hierarchical spectrum with  $m_1 = 10^{-3}$  eV and  $\theta_{13} = 0$ . For the observed oscillation parameters, we take the best fit values of Ref. [37]:

$$\Delta m_{32}^2 \equiv m_3^2 - m_2^2 = 2.4 \times 10^{-3} \text{ eV}^2, \quad \sin^2 \theta_{23} = 0.44, \quad (22)$$

$$\Delta m_{21}^2 \equiv m_2^2 - m_1^2 = 7.92 \times 10^{-5} \text{ eV}^2, \quad \sin^2 \theta_{12} = 0.314. \quad (23)$$

<sup>5</sup>Strictly speaking, Eq. (5) involves the decoupling of four states at scales which can differ by several orders of magnitude. We neglect the associated radiative corrections here and, for simplicity, identify the seesaw scale with the GUT scale in the following.

The Dirac-type phase  $\delta_{PMNS}$  and the two relative Majorana phases contained in  $P_\nu$  are treated as free parameters, as well as the high-energy phases contained in  $P_u$ ,  $P_d$  and  $P_e$ . We denote these phases by  $\Phi_i^{u,d,\nu,e}$ ,  $i = 1, 2, 3$  (some of which are redundant), with  $P_u \equiv \text{Diag}(e^{i\Phi_1^u}, e^{i\Phi_2^u}, e^{i\Phi_3^u})$ ,  $P_d \equiv \text{Diag}(e^{i\Phi_1^d}, e^{i\Phi_2^d}, e^{i\Phi_3^d})$ , and so on.

Fig. 1 shows four out of the eight right-handed neutrino spectra reconstructed from the above inputs as a function of  $v_R$ , assuming  $\beta/\alpha = 0.1$ . The 8 different solutions can be distinguished by the behaviour of each  $M_i$  ( $i = 1, 2, 3$ ) as a function of  $v_R$ . The 4 solutions with  $x_3 = x_3^-$  are characterized by a constant value of the lightest right-handed neutrino mass,  $M_1 \approx 7 \times 10^4$  GeV; among them, the 2 solutions with  $x_2 = x_2^-$  also have  $M_2 \approx 4 \times 10^9$  GeV, while the 2 solutions with  $x_2 = x_2^+$  have a rising  $M_2$ . It is interesting to note that  $7 \times 10^4$  GeV and  $4 \times 10^9$  GeV are nothing but the type I values of  $M_1$  and  $M_2$ , respectively. This is actually not a coincidence, but a direct consequence of Eq. (12): besides the fact that solution  $(-, -, -)$  reduces to the type I case in the large  $v_R$  limit, some of the properties of the type I right-handed neutrino mass spectrum are inherited by the four solutions<sup>6</sup>  $(\pm, \pm', -)$ . The 2 solutions with  $x_3 = x_3^+$  and  $x_2 = x_2^-$ , on the other hand, are characterized by  $M_1 \approx 2 \times 10^9$  GeV, and the 2 solutions with  $x_3 = x_3^+$  and  $x_2 = x_2^+$  by a rising  $M_1$ . In the large  $v_R$  region, solution  $(+, +, +)$  approaches the type II case, as can be seen from the fact that  $M_1 : M_2 : M_3 (\propto f_1 : f_2 : f_3) \propto m_1 : m_2 : m_3$ . It should be stressed that the choice of  $\beta/\alpha$  does not affect the shape of the curves  $M_i = M_i(v_R)$ , but only their position along the horizontal axis. For instance, setting  $\beta/\alpha = 1$  instead of 0.1 would shift the curves in Fig. 1 according to  $v_R \rightarrow \sqrt{0.1} v_R$ . This is due to the fact that, while  $f$  depends on  $\alpha$  and  $\beta$  separately,  $M_R = f v_R$  only depends on the combination  $\alpha\beta$ . In the following we choose  $\beta/\alpha = 0.1$  for numerical convenience, but it should be clear that our results will not depend on this choice.

The implications for leptogenesis of these solutions were discussed in Ref. [29]. Since  $M_\Delta = (\beta/\alpha) \sigma_u v_R / 2 \lesssim (\beta/\alpha) v_R$  and all solutions satisfy  $M_1 \ll v_R$ , one can safely assume that the  $SU(2)_L$  triplet is heavier than the lightest right-handed neutrino. Then the dominant contribution to the lepton asymmetry comes from the out-of-equilibrium decays of  $N_1$  and  $\tilde{N}_1$ , except in some cases where the contribution of  $N_2$  and  $\tilde{N}_2$  actually dominates. One can distinguish between three different behaviours (from now on,  $N_i$  will refer both to the  $i$ th right-handed neutrino and to its supersymmetric partner):

- **solutions  $(\pm, \pm', -)$ :** the four solutions characterized by a low value of  $M_1$  fail to generate the observed baryon asymmetry from  $N_1$  decays. In these solutions, the CP asymmetry in  $N_1$  decays always lies below  $\mathcal{O}(10^{-10})$ , irrespective of the choice of the high-energy phases. This situation is similar to the one encountered in the type I case. In principle,  $N_2$  decays could generate a large asymmetry in a lepton flavour that is only mildly washed out by  $N_1$  decays and inverse decays, thus leading to successful leptogenesis [23]. Estimates of this effect tend to show, however, that it is unlikely to work in solution  $(-, -, -)$ .
- **solutions  $(\pm, +, +)$ :** in the two solutions characterized by a rising  $M_1$ , the CP asymmetry in  $N_1$  decays grows with  $v_R$ . Successful leptogenesis then becomes possible for large values of  $v_R$ , i.e. in the region where the type II seesaw contribution dominates in the light neutrino mass matrix. However, one finds a tension between successful leptogenesis, which requires  $M_1 \gtrsim 10^{10}$  GeV, and the gravitino overproduction problem [38], which imposes an upper bound  $T_{RH} \lesssim (10^9 - 10^{10})$  GeV on the reheating temperature [39].
- **solutions  $(\pm, -, +)$ :** the two solutions characterized by  $M_1 \sim 10^9$  GeV can lead to a relatively large CP asymmetry in  $N_1$  decays without conflicting with the gravitino constraint. However, the washout of the generated lepton asymmetry by lepton number violating processes tends to be large. To determine whether the observed baryon asymmetry can indeed be generated, one must integrate numerically the Boltzmann equations.

<sup>6</sup>A comment about our notation might be necessary: the prime symbol in  $\pm'$  means that the second sign in  $(\pm, \pm', -)$  is not correlated with the first one, i.e.  $(\pm, \pm', -)$  refers to the four solutions  $(+, +, -)$ ,  $(+, -, -)$ ,  $(-, +, -)$  and  $(-, -, -)$ .

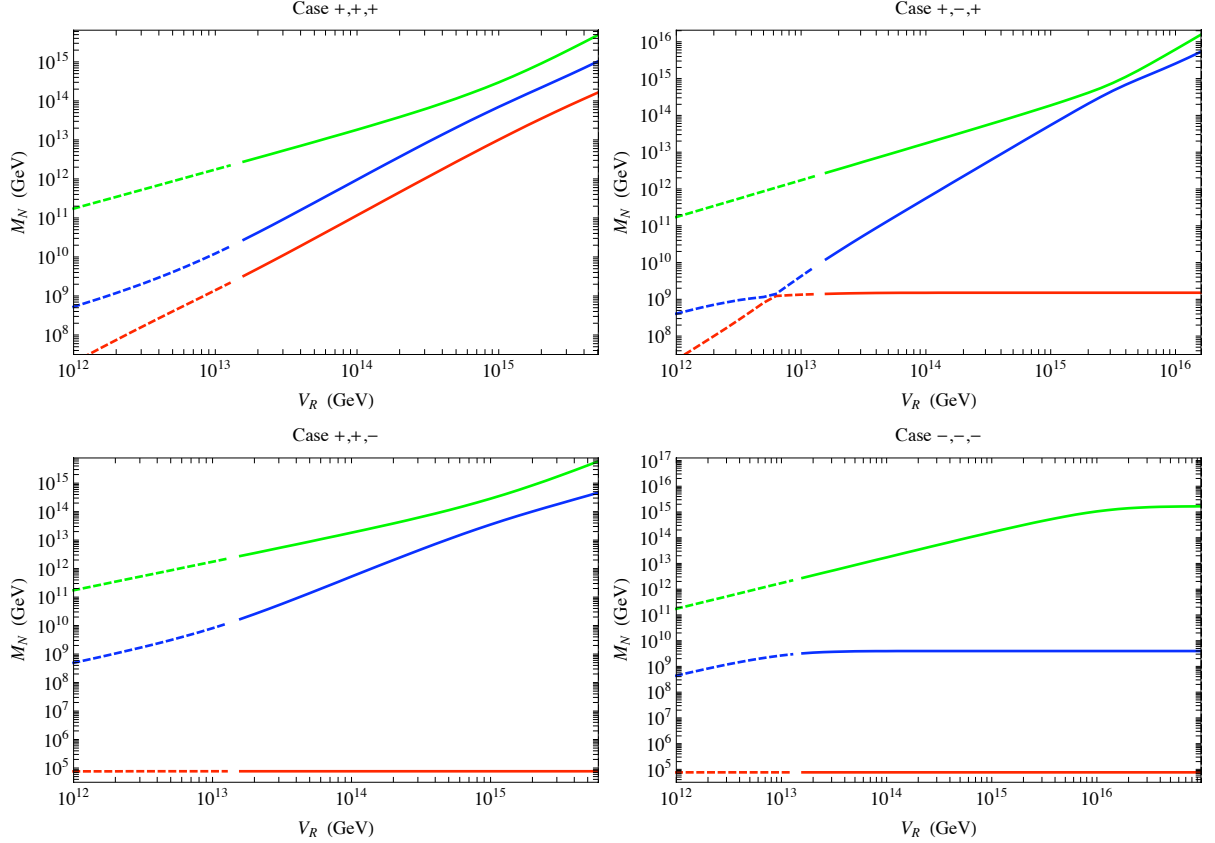


Figure 1: Right-handed neutrino masses as a function of  $v_R$  in solutions  $(+, +, +)$ ,  $(+, -, +)$ ,  $(+, -, -)$  and  $(-, -, -)$ . Inputs: hierarchical light neutrino masses with  $m_1 = 10^{-3}$  eV, oscillation parameters as specified in the text, and no CP violation besides the CKM phase ( $\delta_{PMNS} = \Phi_i^u = \Phi_i^d = \Phi_i^\nu = \Phi_i^e = 0$ );  $\beta/\alpha = 0.1$ . The range of variation of  $v_R$  is restricted from above by the requirement that  $|f_{ij}| \leq 1$ . Dashed lines indicate a cancellation at a stronger level than 1% between the type I and type II contributions to the light neutrino mass matrix.

A general feature of all solutions is that lepton number violating processes tend to efficiently wash out the generated lepton asymmetry. This can be traced back to the relation  $M_D = M_u$ , which implies that at least one of the Dirac couplings is of the order of the top quark Yukawa coupling. As a consequence, predictions for leptogenesis depend on the details of the dynamics encoded in the Boltzmann equations.

It is clear from the above discussion that, for most solutions, the qualitative analysis of Ref. [29] is not sufficient to tell whether leptogenesis can indeed be successful. The purpose of the present paper is to perform a careful, quantitative study of leptogenesis in supersymmetric  $SO(10)$  models with a left-right symmetric seesaw mechanism, taking into account the lepton flavour dynamics [40]–[53], as well as the contribution of the next-to-lightest right-handed neutrino supermultiplet [22, 23, 52, 54, 55]. As is well known from studies performed in the type I case, flavour effects can significantly enhance the final baryon asymmetry if there is a hierarchy between the washout parameters for different lepton flavours [41, 42, 43], and their impact might be crucial for solutions  $(\pm, \pm', -)$  and  $(\pm, -, +)$ . Furthermore, the contribution of the next-to-lightest right-handed (s)neutrino can be relevant both for  $M_1 \approx M_2$  and for  $M_1 \ll M_2$ , provided in the latter case that  $N_1$ -related washout effects are weak. The Boltzmann equations including all these ingredients will be presented in the next section. Finally, the corrections to the GUT-scale mass relation  $M_d = M_e$  needed to account for the measured down quark and charged lepton masses will modify the reconstructed seesaw parameters and affect the final baryon asymmetry. These effects will be taken into account in Section 4.

### 3 Boltzmann equations

In this section, we write the Boltzmann equations that govern thermal leptogenesis in the class of supersymmetric  $SO(10)$  models described above. The relevant heavy degrees of freedom are the three right-handed neutrinos  $N_{1,2,3}$  and the scalar Higgs triplet  $\Delta$ , as well as their supersymmetric partners. In principle, all these states could contribute to the generation of the lepton asymmetry through their decays. However, due to the strong hierarchy among their masses, only the decays of  $N_1$  and  $N_2$  and of their scalar partners are relevant in practice<sup>7</sup>.

Let us first consider the CP asymmetries in heavy (s)neutrino decays. The relevant superpotential terms, written in the basis of charged lepton and right-handed neutrino mass eigenstates, read:

$$W_{seesaw} = \lambda_{i\alpha} N_i^c L_\alpha^T i\sigma^2 H_u + \frac{1}{2} M_i N_i^c N_i^c + \frac{1}{2} f_{\alpha\beta} L_\alpha^T i\sigma^2 \Delta L_\beta + \frac{1}{2} \sigma_u H_u^T i\sigma^2 \bar{\Delta} H_u + M_\Delta \text{Tr}(\Delta \bar{\Delta}), \quad (24)$$

where  $N_i^c$ ,  $L_\alpha$  and  $H_u$  are the right-handed neutrino, lepton doublet and Higgs doublet superfields, respectively, and

$$\Delta \equiv \frac{\vec{\sigma}}{\sqrt{2}} \cdot \vec{\Delta} = \begin{pmatrix} \Delta^+/\sqrt{2} & \Delta^{++} \\ \Delta^0 & -\Delta^+/\sqrt{2} \end{pmatrix}, \quad \bar{\Delta} \equiv \frac{\vec{\sigma}}{\sqrt{2}} \cdot \vec{\bar{\Delta}} = \begin{pmatrix} \bar{\Delta}^-/\sqrt{2} & \bar{\Delta}^0 \\ \bar{\Delta}^{--} & -\bar{\Delta}^-/\sqrt{2} \end{pmatrix}. \quad (25)$$

Being Majorana particles, the heavy neutrinos can decay both into  $\ell_\alpha H_u$  (lepton + Higgs boson),  $\tilde{\ell}_\alpha \tilde{H}_u$  (slepton + higgsino) and into the CP-conjugated final states  $\bar{\ell}_\alpha H_u^*$  and  $\tilde{\ell}_\alpha^* \tilde{H}_u$ . Their scalar partners  $\tilde{N}_i^c$  are not CP eigenstates and have only 2 two-body decay modes,  $\tilde{N}_i^c \rightarrow \bar{\ell}_\alpha \tilde{H}_u$  and  $\tilde{N}_i^c \rightarrow \tilde{\ell}_\alpha H_u$ . The corresponding tree-level decay rates are [56]:

$$\Gamma(N_i \rightarrow \ell_\alpha H_u) = \Gamma(N_i \rightarrow \bar{\ell}_\alpha H_u^*) = \Gamma(N_i \rightarrow \tilde{\ell}_\alpha \tilde{H}_u) = \Gamma(N_i \rightarrow \tilde{\ell}_\alpha^* \tilde{H}_u) = \frac{M_i}{16\pi} |\lambda_{i\alpha}|^2, \quad (26)$$

$$\Gamma(\tilde{N}_i^c \rightarrow \bar{\ell}_\alpha \tilde{H}_u) = \Gamma(\tilde{N}_i^c \rightarrow \tilde{\ell}_\alpha H_u) = \frac{M_i}{8\pi} |\lambda_{i\alpha}|^2. \quad (27)$$

Supersymmetry implies the equality of the total decay widths,  $\Gamma_{N_i} = \Gamma_{\tilde{N}_i^c} = M_i(\lambda\lambda^\dagger)_{ii}/4\pi$ . At the one-loop level, an asymmetry between CP-conjugated decay channels arises from the interference of tree-level and one-loop Feynman diagrams. One can define 4 different types of flavour-dependent CP asymmetries which, due to supersymmetry, are given by the same quantities  $\epsilon_{i\alpha}$ :

$$\begin{aligned} \epsilon_{i\alpha} &\equiv \frac{\Gamma(N_i \rightarrow \ell_\alpha H_u) - \Gamma(N_i \rightarrow \bar{\ell}_\alpha H_u^*)}{\Gamma(N_i \rightarrow \ell H_u) + \Gamma(N_i \rightarrow \bar{\ell} H_u^*)} = \frac{\Gamma(N_i \rightarrow \tilde{\ell}_\alpha \tilde{H}_u) - \Gamma(N_i \rightarrow \tilde{\ell}_\alpha^* \tilde{H}_u)}{\Gamma(N_i \rightarrow \tilde{\ell} \tilde{H}_u) + \Gamma(N_i \rightarrow \tilde{\ell}^* \tilde{H}_u)} \\ &= \frac{\Gamma(\tilde{N}_i^c \rightarrow \bar{\ell}_\alpha \tilde{H}_u) - \Gamma(\tilde{N}_i^{c*} \rightarrow \tilde{\ell}_\alpha H_u)}{\Gamma(\tilde{N}_i^c \rightarrow \bar{\ell} \tilde{H}_u) + \Gamma(\tilde{N}_i^{c*} \rightarrow \tilde{\ell} H_u)} = \frac{\Gamma(\tilde{N}_i^c \rightarrow \tilde{\ell}_\alpha H_u) - \Gamma(\tilde{N}_i^{c*} \rightarrow \tilde{\ell}_\alpha^* H_u)}{\Gamma(\tilde{N}_i^c \rightarrow \tilde{\ell} H_u) + \Gamma(\tilde{N}_i^{c*} \rightarrow \tilde{\ell}^* H_u)}, \end{aligned} \quad (28)$$

where  $\Gamma(N_i \rightarrow \ell H_u) \equiv \sum_\beta \Gamma(N_i \rightarrow \ell_\beta H_u)$ , etc. The  $\epsilon_{i\alpha}$ 's receive both a type I contribution (right-handed neutrino-induced vertex and self-energy corrections) and a type II contribution (triplet-induced vertex correction):

$$\epsilon_{i\alpha} = \epsilon_{i\alpha}^I + \epsilon_{i\alpha}^{II}. \quad (29)$$

The type I contribution reads [56]:

$$\epsilon_{i\alpha}^I = \frac{1}{8\pi} \sum_{j \neq i} \frac{\text{Im}[\lambda_{i\alpha}(\lambda\lambda^\dagger)_{ij} \lambda_{j\alpha}^*]}{(\lambda\lambda^\dagger)_{ii}} f_I \left( \frac{M_j^2}{M_i^2} \right), \quad (30)$$

<sup>7</sup>Indeed, all solutions satisfy  $M_{1,2} \ll M_3, M_\Delta$  over a large range of values for  $v_R$  (assuming  $M_\Delta \sim (\beta/\alpha)v_R$  and  $\beta/\alpha$  not too small), hence the lepton asymmetry generated in  $\Delta$  and  $N_3$  decays is washed out by  $N_2$ - and  $N_1$ -related processes. In the large  $v_R$  region of some solutions, one has instead  $M_2 \sim M_3$  ( $M_\Delta$ ), but  $N_2$  and  $N_3$  ( $\Delta$ ) turn out to be too heavy to be thermally produced after reheating. Indeed, one typically has  $M_2 > 10^{12}$  GeV in this case, while the upper bound on the reheating temperature associated with the gravitino overproduction problem is  $\mathcal{O}(10^9 - 10^{10})$  GeV.

while the type II contribution is given by [57, 58]:

$$\epsilon_{i\alpha}^{II} = \frac{3}{8\pi} \sum_{\beta} \frac{\text{Im}[\lambda_{i\beta}(M_{\nu}^{II})_{\beta\alpha}^* \lambda_{i\alpha}]}{(\lambda\lambda^{\dagger})_{ii}} \frac{M_i}{v_u^2} f_{II}\left(\frac{M_{\Delta}^2}{M_i^2}\right). \quad (31)$$

In Eqs. (30) and (31), the loop functions are given by:

$$f_I(x) = \sqrt{x} \left( \frac{2}{1-x} - \ln\left(\frac{1+x}{x}\right) \right) \xrightarrow{x \gg 1} -\frac{3}{\sqrt{x}}, \quad (32)$$

$$f_{II}(y) = y \ln\left(\frac{1+y}{y}\right) \xrightarrow{y \gg 1} 1. \quad (33)$$

Eqs. (30) and (32) are valid for hierarchical right-handed neutrinos; in the case of a partial degeneracy,  $M_1 \simeq M_2 \ll M_3$ , they must be modified. Following Ref. [59], we take:

$$\epsilon_{i\alpha}^I = \frac{1}{8\pi} \frac{1}{(\lambda\lambda^{\dagger})_{ii}} \sum_{j \neq i} \text{Im} \left( \lambda_{i\alpha} \lambda_{j\alpha}^* \left\{ (\lambda\lambda^{\dagger})_{ij} (C_v^{ij} + 2C_{s,a}^{ij}) + (\lambda\lambda^{\dagger})_{ji} 2C_{s,b}^{ij} \right\} \right), \quad (34)$$

where  $C_v^{ij}$ ,  $C_{s,a}^{ij}$  and  $C_{s,b}^{ij}$  are functions of  $M_j^2/M_i^2$ .  $C_v^{ij}$  is the usual vertex function:

$$C_v^{ij}(x) = -\sqrt{x} \ln\left(\frac{1+x}{x}\right), \quad (35)$$

while  $C_{s,a}^{ij}$  and  $C_{s,b}^{ij}$  arise from self-energy corrections:

$$C_{s,a}^{ij}(x) = \sqrt{x} C_{s,b}^{ij}(x) = \frac{\sqrt{x}(1-x)}{(1-x)^2 + x(\lambda\lambda^{\dagger})_{jj}^2/16\pi^2}. \quad (36)$$

The term proportional to  $C_{s,b}^{ij}$  in Eq. (34) does not contribute to the total CP asymmetry in  $N_i$  decays and is therefore a pure flavour effect [56]. In the limit of hierarchical right-handed neutrinos,  $x \gg 1$ , this term can be neglected and  $C_{s,a}^{ij}(x) \simeq \sqrt{x}/(1-x)$ . One then recovers the non-resonant formula (30).

The strength of the processes involving  $\bar{N}_i$  ( $\widetilde{N}_i^c$ ) and  $\ell_{\alpha}$  ( $\widetilde{\ell}_{\alpha}$ ) is parametrized by individual washout parameters<sup>8</sup>  $\kappa_{i\alpha}$ :

$$\kappa_{i\alpha} \equiv \frac{\Gamma(N_i \rightarrow \ell_{\alpha} H_u) + \Gamma(N_i \rightarrow \bar{\ell}_{\alpha} H_u^*)}{H(M_i)}. \quad (37)$$

Defining the effective neutrino masses

$$\tilde{m}_{i\alpha} \equiv \frac{|\lambda_{i\alpha}|^2 v_u^2}{M_i}, \quad (38)$$

the individual washout parameters  $\kappa_{i\alpha}$  can be expressed as

$$\kappa_{i\alpha} = \frac{\tilde{m}_{i\alpha}}{m_*}, \quad (39)$$

where  $m_* = 16\pi^{5/2} \sqrt{g_*} v_u^2 / (3\sqrt{5} M_P) \simeq (1.56 \times 10^{-3} \text{eV}) \sin^2 \beta$  is the equilibrium neutrino mass (we used the fact that the number of effectively massless degrees of freedom in the thermal bath at  $T = M_1$  is  $g_* = 228.75$  in the MSSM). Summing over flavour indices, one obtains the total washout parameters  $\kappa_i$ :

$$\kappa_i = \sum_{\alpha} \kappa_{i\alpha} = \frac{\tilde{m}_i}{m_*} \simeq \frac{\tilde{m}_i}{(1.56 \times 10^{-3} \text{eV}) \sin^2 \beta}. \quad (40)$$

<sup>8</sup>We follow here the notations and conventions of Refs. [43, 60].

The out-of-equilibrium condition for  $N_i$  decays (resp.  $N_i$  decays into  $\ell_\alpha$  or  $\bar{\ell}_\alpha$ ) reads  $\kappa_i < 1$  (resp.  $\kappa_{i\alpha} < 1$ ). If  $N_i$  is in the strong washout regime ( $\kappa_i \gg 1$ ), scattering processes in the thermal bath produce an equilibrium population of  $N_i$  at  $T \sim M_i$ . When  $T$  drops below  $M_i$ , the  $N_i$  decay and generate asymmetries in all lepton flavours, in proportions controlled by the  $\epsilon_{i\alpha}$ ,  $\alpha = e, \mu, \tau$ . Assuming that the decays occur in the temperature regime where all flavours are relevant, the dynamical evolution of the individual flavour asymmetries depends on the  $\kappa_{j\alpha}$ , where the index  $j$  runs over the  $N_j$  such that  $M_j \lesssim M_i$ . If  $\kappa_{j\alpha} \gg 1$ , the asymmetry in the lepton flavour  $\alpha$  is strongly washed out by the lepton number violating processes involving  $N_j$ , which are in equilibrium at  $T = M_j$ ; if  $\kappa_{j\alpha} \ll 1$ , the opposite is true. Consider now the case where  $N_i$  is in the weak washout regime ( $\kappa_i \ll 1$ ). Then its number density never reaches thermal equilibrium, but since  $\kappa_{i\alpha} \ll 1$  for all  $\alpha$ , the individual flavour asymmetries are only weakly washed out by  $N_i$ -related processes (they may however be strongly washed out by  $N_j$ -related processes,  $j \neq i$ ).

The evolution of the number densities is obtained by solving the set of Boltzmann equations. As is usual done, we take into account the expansion of the universe by defining comoving number densities  $Y_X \equiv n_X/s$ . The supersymmetric Boltzmann equations for the heavy (s)neutrino comoving number densities read [61]:

$$Y'_{N_i}(z) = -2 \kappa_i (D_i(z) + S_i(z)) \left( Y_{N_i}(z) - Y_{N_i}^{eq}(z) \right), \quad (41)$$

$$Y'_{\tilde{N}_i}(z) = -2 \kappa_i (D_i(z) + S_i(z)) \left( Y_{\tilde{N}_i}(z) - Y_{\tilde{N}_i}^{eq}(z) \right), \quad (42)$$

where  $Y_{\tilde{N}_i}$  stands for  $Y_{\tilde{N}_i^c} + Y_{\tilde{N}_i^{c\dagger}}$ ,  $z \equiv M_1/T$  and the symbol  $'$  stands for  $d/dz$ . The equilibrium densities appearing in Eqs. (41) and (42) are given by:

$$Y_{N_i}^{eq}(z) = \frac{135\zeta(3)}{8\pi^4 g_*} R_i^2 z^2 K_2(R_i z) \xrightarrow{T \gg M_i} \frac{135\zeta(3)}{4\pi^4 g_*} \simeq 1.8 \times 10^{-3}, \quad (43)$$

$$Y_{\tilde{N}_i}^{eq}(z) = \frac{4}{3} Y_{N_i}^{eq}(z), \quad (44)$$

where  $R_i \equiv M_i/M_1$ , and we have corrected the high temperature behaviour of the Maxwell-Boltzmann distribution by a factor of  $3\zeta(3)/4$  in  $Y_{N_i}^{eq}(z)$ , and by a factor of  $\zeta(3)$  in  $Y_{\tilde{N}_i}^{eq}(z)$ <sup>9</sup>. The factor of 2 in the right-hand side of Eqs. (41) and (42) accounts for the fact that there are twice as many channels in the supersymmetric case as in the non-supersymmetric case. In the regime in which all lepton flavours are relevant, the individual  $\Delta_\alpha \equiv B/3 - L_\alpha$  asymmetries are driven by the following Boltzmann equations [43, 45]:

$$\begin{aligned} Y'_{\Delta_\alpha}(z) &= -2 \sum_{i=1,2} \epsilon_{i\alpha} \kappa_i (D_i(z) + S_i(z)) \left( Y_{N_i}(z) - Y_{N_i}^{eq}(z) + \left( Y_{\tilde{N}_i}(z) - Y_{\tilde{N}_i}^{eq}(z) \right) \right) \\ &+ 2 \sum_{i=1,2} \kappa_{i\alpha} \sum_{\beta} W_i(z) A_{\alpha\beta} Y_{\Delta_\beta}(z), \end{aligned} \quad (45)$$

where  $Y_{\Delta_\alpha}$  stands for the total  $\Delta_\alpha$  asymmetry stored in the fermionic species and in their supersymmetric partners. In Eqs. (41), (42) and (45), the thermally averaged decay rates  $D_i(z)$  are given by:

$$D_i(z) = R_i^2 z \frac{K_1(R_i z)}{K_2(R_i z)}. \quad (46)$$

<sup>9</sup>Assuming Maxwell-Boltzmann (MB) statistics as is customary, the equilibrium number density at high temperature differs from the Fermi-Dirac (FD) and Bose-Einstein (BE) cases by a numerical factor:

$$n_{FD}(T \gg M) = \frac{3}{4} n_{BE}(T \gg M) = \frac{3\zeta(3)}{4} n_{MB}(T \gg M),$$

while  $n_{FD}(T) \simeq n_{BE}(T) \simeq n_{MB}(T)$  at low temperature ( $T \ll M$ ).

The scatterings terms  $S_i(z)$  account for Higgs-mediated  $\Delta L = 1$  scatterings involving top quarks and antiquarks. They receive both s- and t-channel contributions:

$$S_i(z) = 2S_s^i(z) + 4S_t^i(z), \quad (47)$$

whose expression can be found in Ref. [60]. The washout term  $W_i(z) = W_i^{ID}(z) + W_i^S(z)$  results from the contribution of inverse decays:

$$W_i^{ID}(z) = \frac{1}{4} R_i^4 z^3 K_1(R_i z), \quad (48)$$

and  $\Delta L = 1$  scatterings [60]:

$$W_i^S(z) = \frac{W_i^{ID}(z)}{D_i(z)} \left( 2S_s^i(z) \left( \frac{Y_{N_i}(z)}{Y_{N_i}^{eq}(z)} + \frac{Y_{\tilde{N}_i}(z)}{Y_{\tilde{N}_i}^{eq}(z)} \right) + 8S_t^i(z) \right). \quad (49)$$

In writing the above Boltzmann equations, we made several assumptions which we now proceed to clarify. In the washout term, we neglected the off-shell part of the  $\Delta L = 2$  scatterings, which is a good approximation as long as  $M_i \ll \kappa_{i\alpha} (10^{13} \text{ GeV})$  [43]. We also omitted  $\Delta L = 0$  scatterings such as  $N_i N_j \rightarrow \ell \bar{\ell}$ ,  $N_i N_j \rightarrow H_u H_u^*$  and  $N_i \ell(\bar{\ell}) \rightarrow N_j \ell(\bar{\ell})$ , which do not contribute to the washout but can affect the abundance of the heavy (s)neutrinos (when flavour effects are taken into account, they also tend to redistribute the lepton asymmetry among flavours). These processes are of higher order in the neutrino Yukawa couplings and are expected to have little impact on the final baryon asymmetry. We further neglected the triplet-related washout processes, gauge scatterings [8, 59], spectator processes [9], and the higher order processes  $1 \rightarrow 3$  and  $2 \rightarrow 3$  [62]. Finally, since the left-right symmetry is broken at a scale  $v_R$  which may lie several orders of magnitude below  $M_{GUT}$ , one may worry that decay and scattering processes mediated by the heavy  $SU(2)_R \times U(1)_{B-L}$  gauge bosons affect the heavy (s)neutrino number densities. Indeed,  $W_R$ - and  $Z'$ -mediated processes such as  $N_i e_R \rightarrow \bar{q}_R q'_R$  and  $N_i N_i \rightarrow f \bar{f}$  tend to keep the heavy (s)neutrinos in thermal equilibrium, thus reducing the generated lepton asymmetry [63, 64]. As shown in Ref. [65], however, this effect can be practically neglected if  $M_i/v_R < 10^{-2}$ , which turns out to be the case for  $i = 1, 2$  in each of the 8 solutions (at least as long as  $N_{1,2}$  are light enough to be thermally produced after reheating, i.e.  $M_{1,2} \lesssim 10^{11} \text{ GeV}$ ). Therefore, we do not need to include  $W_R$ - and  $Z'$ -mediated processes in our study<sup>10</sup>.

The Boltzmann equations (45) are written for the  $B/3 - L_\alpha$  asymmetries  $Y_{\Delta_\alpha}$  rather than for the lepton asymmetries  $Y_{L_\alpha}$ , because the former are preserved by all MSSM interactions (including the non-perturbative sphaleron processes), contrary to the latter. As the washout term in Eq. (45) depends on  $Y_{L_\alpha}$ , we need to express it in terms of the  $Y_{\Delta_\beta}$ 's. This is done by a conversion matrix  $A$  [10], whose entries depend on which interactions are in equilibrium:

$$Y_{L_\alpha} = \sum_{\beta} A_{\alpha\beta} Y_{\Delta_\beta}. \quad (50)$$

Depending on the temperature at which leptogenesis takes place (identified for simplicity with  $M_1$  below), one must consider one of the following three regimes. If  $M_1 \lesssim 10^9 \text{ GeV}$  ( $1 + \tan^2 \beta$ ), the tau and muon Yukawa interactions are in equilibrium, hence all three lepton flavours are distinguishable. One must then write three separate Boltzmann equations for the flavour asymmetries  $Y_{\Delta_e}$ ,  $Y_{\Delta_\mu}$  and  $Y_{\Delta_\tau}$ , as in Eq. (45). The  $3 \times 3$   $A$  matrix is given by [45]:

$$A = \begin{pmatrix} -93/110 & 6/55 & 6/55 \\ 3/40 & -19/30 & 1/30 \\ 3/40 & 1/30 & -19/30 \end{pmatrix}. \quad (51)$$

<sup>10</sup>Note however that  $W_R$ - and  $Z'$ -mediated scatterings can help generating an equilibrium population of  $N_i$  in the weak washout regime ( $\kappa_i \ll 1$ ), provided that  $M_i/v_R > 10^{-3}$  [65].

If  $10^9 \text{ GeV} (1 + \tan^2 \beta) \lesssim M_1 \lesssim 10^{12} \text{ GeV} (1 + \tan^2 \beta)$ , the muon Yukawa interactions are no longer in equilibrium, and the electron and muon lepton flavours can no longer be distinguished. The lepton asymmetry must then be projected onto the 2-flavour space  $(Y_{L_{e+\mu}}, Y_{L_\tau})$ , where  $Y_{L_{e+\mu}} \equiv Y_{L_e} + Y_{L_\mu}$ , and correspondingly  $Y_{\Delta_{e+\mu}} \equiv Y_{\Delta_e} + Y_{\Delta_\mu}$ . The conversion matrix is now a  $2 \times 2$  matrix:

$$A = \begin{pmatrix} -541/761 & 152/761 \\ 46/761 & -494/761 \end{pmatrix}, \quad (52)$$

and the Boltzmann equations for  $Y_{\Delta_e}$  and  $Y_{\Delta_\mu}$  must be replaced by a single equation for  $Y_{\Delta_{e+\mu}}$  involving the CP asymmetries  $\epsilon_{i,e+\mu} \equiv \epsilon_{ie} + \epsilon_{i\mu}$  and the washout parameters  $\kappa_{i,e+\mu} \equiv \kappa_{ie} + \kappa_{i\mu}$ . Finally, if  $M_1 \gtrsim 10^{12} \text{ GeV} (1 + \tan^2 \beta)$ , none of the interactions involving charged lepton Yukawa couplings are in equilibrium, and one recovers the flavour-independent treatment of leptogenesis with  $A = -\mathbb{1}$ .

It has been pointed out in Ref. [49] that the out-of-equilibrium condition used above to determine the flavour regime is actually not sufficient. For a given flavour asymmetry  $Y_{\Delta_\alpha}$  to evolve independently during leptogenesis, the corresponding charged lepton Yukawa interaction rate  $\Gamma_\alpha(T) \simeq 5 \times 10^{-3} h_\alpha^2 (1 + \tan^2 \beta) T$  should not only be faster than the expansion rate of the Universe, but, more importantly, it should also be faster than the  $N_i$  inverse decay rate. If this were not the case, inverse decays would keep the evolution of the lepton state coherent. For the tau and muon lepton flavours, this condition reads  $M_1 \lesssim 10^{12} \text{ GeV} (1 + \tan^2 \beta) / \kappa_{1\tau}$  and  $M_1 \lesssim 10^9 \text{ GeV} (1 + \tan^2 \beta) / \kappa_{1\mu}$ , respectively. It is more restrictive than the out-of-equilibrium condition for  $\kappa_{1\tau} \gg 1$  (resp.  $\kappa_{1\mu} \gg 1$ ).

The final baryon asymmetry is given by:

$$Y_B = \frac{10}{31} \sum_\alpha Y_{\Delta_\alpha}, \quad (53)$$

where the factor  $10/31$  is due to the partial conversion of the  $\Delta_\alpha$  asymmetries into a baryon asymmetry by the non-perturbative sphaleron processes [4] (we assume here that sphalerons come out of thermal equilibrium below the electroweak phase transition). It has been pointed out recently [66] that the conversion factors relating the flavour asymmetries  $Y_{\Delta_\alpha}$  to  $Y_B$  depend on the actual superpartner spectrum. Strictly speaking, Eq. (53) is only valid if all sfermions are heavy, while the final baryon asymmetry can be reduced by a factor of  $2/3$  if sleptons are light, as in some minimal supergravity scenarios. Since we do not assume any particular superpartner spectrum in this paper, we shall stick to Eq. (53) in the following.

Being supersymmetric, the Grand Unified models we are considering in this paper face the so-called gravitino problem [38]: in an inflationary universe, gravitinos are abundantly produced by thermal scatterings in the reheating phase and, if they are unstable, their late decays tend to spoil the successful predictions of Big Bang nucleosynthesis. The requirement that this does not happen puts an upper bound on the reheating temperature,  $T_{RH} \lesssim (10^5 - 10^{10}) \text{ GeV}$  for  $300 \text{ GeV} \lesssim m_{3/2} \lesssim 30 \text{ TeV}$ , depending on the gravitino mass and on the superparticle spectrum [67]. If instead the gravitino is the lightest supersymmetric particle (LSP), the requirement that its relic density does not exceed the dark matter abundance leads to a weaker constraint,  $T_{RH} \lesssim (10^9 - 10^{10}) \text{ GeV}$  for a gravitino of mass  $m_{3/2} \sim 100 \text{ GeV}$  [39]. These constraints are in conflict with successful thermal leptogenesis, which requires  $M_1 \gtrsim 10^9 \text{ GeV}$  in the type I seesaw case [6]. In the left-right symmetric seesaw case studied in this paper, we also find such a tension. We nevertheless stick to thermal leptogenesis, since some supersymmetric scenarios can accommodate a reheating temperature  $T_{RH} \sim 10^{10} \text{ GeV}$  (see the discussion at the end of Section 5). In our numerical computation of the baryon asymmetry, we do not explicitly include the dynamics of reheating in the Boltzmann equations, as was done in Refs. [8, 48, 68], but we take the reheating temperature into account in the initial conditions. Namely, we start evolving the Boltzmann equations at some temperature  $T_{in}$ , which we identify with  $T_{RH}$ . Heavy (s)neutrinos with masses  $M_i \gtrsim (4-5) T_{in}$  will thus give a negligible contribution to the lepton asymmetry, because their production processes (inverse decays and  $\Delta L = 1$  scatterings) are Boltzmann-suppressed.

## 4 Numerical results

In this section, we present our numerical results for leptogenesis in the class of supersymmetric  $SO(10)$  models described in Section 2. The final baryon asymmetry is obtained by numerically integrating the Boltzmann equations written in Section 3, starting the evolution at  $T_{in} = 10^{11}$  GeV with vanishing abundances for  $N_{1,2}$  and  $\tilde{N}_{1,2}$ . With this choice of  $T_{in}$  and  $\tan\beta = 10$ , one can consider that leptogenesis always takes place in the 3-flavour regime. In Section 5, we shall investigate the effect of lowering  $T_{in}$ .

We present results for the following four reference solutions:

- (+, +, +): this solution, which corresponds to dominance of the type II seesaw contribution in the large  $v_R$  region, is characterized by a mild hierarchy of right-handed neutrino masses, with  $M_{1,2}$  growing with  $v_R$ .
- (+, -, +): this solution is characterized by an intermediate value of  $M_1$  ( $M_1 \sim 10^{9-10}$  GeV).
- (-, -, -): this solution, which reduces to the type I seesaw case in the limit  $v_R \rightarrow \infty$ , is characterised by a hierarchical right-handed neutrino mass spectrum with a small value of  $M_1$  ( $M_1 \sim 10^{4-5}$  GeV) and an intermediate value of  $M_2$ .
- (+, +, -): this solution differs from the previous one by the fact that  $M_2$  grows with  $v_R$  rather than assuming a constant value.

The four remaining solutions show very similar patterns of right-handed neutrino masses (the main differences are in the behaviour of  $M_2$  and  $M_3$  in the large  $v_R$  region) and give analogous results for the baryon asymmetry. The input values for the quark masses and mixing angles and for the measured neutrino oscillation parameters are chosen as specified in Section 2. We further assume a hierarchical light neutrino mass spectrum with  $m_1 = 10^{-3}$  eV and  $\theta_{13} = 0$ ; in Section 5, we shall study the effect of varying these input parameters. Rather than attempting to perform a scan over the large number of available CP-violating phases, we choose specific values for these phases in order to illustrate the typical behaviour of the different solutions. We first show the results obtained under the assumption that  $M_d = M_e$  holds at the GUT scale; in a second stage, we include the necessary corrections to this mass relation and investigate their effects on the right-handed neutrino mass spectrum and on the final baryon asymmetry. Finally, we set  $\beta/\alpha = 0.1$  for practical reasons of numerical integration. As explained in Section 2.3, changing the value of  $\beta/\alpha$  only amounts to shift the curves along the  $v_R$  axis.

For convenience, we shall plot the absolute value of the baryon asymmetry  $|Y_B|$  rather than  $Y_B$  itself. Since the sign of  $Y_B$  can be reverted by simply changing the sign of all CP-violating phases, we do not lose any information by doing so, at least to the extent that the effect of the CKM phase (whose sign is determined experimentally) can be neglected. In practice this will be the case in all examples studied in this paper, because the CKM phase always appears in combination with small quark mixing angles, and large high-energy phases are assumed to be present.

### 4.1 Relevance of flavour effects

We first show in Fig. 2 the final baryon asymmetry in the absence of corrections to the GUT-scale mass relation  $M_d = M_e$ , for the four reference solutions (+, +, +), (+, -, +), (+, +, -) and (-, -, -). In order to estimate the relevance of flavour effects, we plotted the result of the numerical computation both in the one-flavour approximation (dashed black line) and in the flavour-dependent approach (solid red line). One can see that flavour effects tend to enhance the baryon asymmetry by up to one order of magnitude in the (+, +, +) and (+, -, +) cases. Not surprisingly, solution (+, +, +) leads to successful leptogenesis for large values<sup>11</sup> of  $v_R$ , where  $M_1 \gtrsim 10^{10}$  GeV; flavour effects allow this solution to be

<sup>11</sup>We do not show the region  $v_R > 2 \times 10^{14}$  GeV, where  $Y_B$  drops below the WMAP value. This behaviour is due to the fact that, above  $v_R = \text{few} \times 10^{14}$  GeV,  $N_1$  and  $N_2$  are too heavy to be thermally produced ( $M_{1,2} \gg T_{in}$ ).

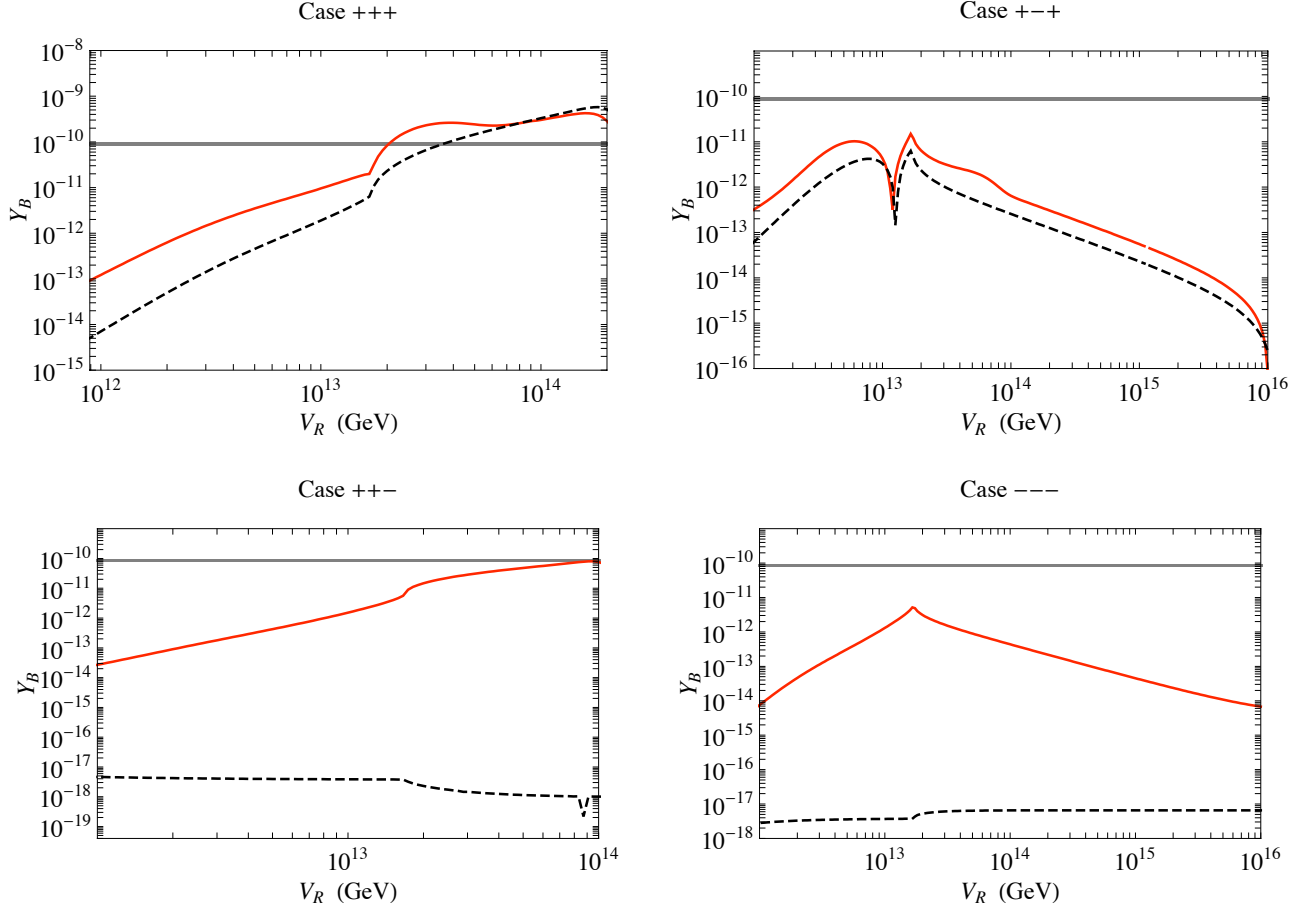


Figure 2: The final baryon asymmetry as a function of  $v_R$  for the four reference solutions, in the one-flavour approximation (dashed black line) and with flavour effects taken into account (solid red line). The GUT-scale mass relation  $M_d = M_e$  is assumed. Inputs: hierarchical light neutrino masses with  $m_1 = 10^{-3}$  eV,  $\theta_{13} = 0$  and no CP violation in the PMNS mixing matrix;  $\Phi_2^u = \pi/4$  and all other high-energy phases are set to zero;  $\beta/\alpha = 0.1$ . The Boltzmann equations are evolved starting from  $T_{in} = 10^{11}$  GeV. The thick horizontal line corresponds to the WMAP constraint.

successful for smaller values of  $v_R$  (i.e. for smaller values of  $M_1$ ) than in the one-flavour approximation. By contrast, solution  $(+, -, +)$  fails to generate the observed baryon asymmetry due to the strong washout by inverse decays and  $\Delta L = 1$  scatterings, and this conclusion still holds for different choices of the CP-violating phases.

Flavour effects have a much more dramatic impact in the  $(+, +, -)$  and  $(-, -, -)$  cases, which are characterized by a strong hierarchy between  $M_1$  and  $M_2$ . In these solutions, the observed enhancement of  $Y_B$  is due to the fact that the asymmetry in a particular lepton flavour is only mildly washed out by  $N_1$ -related processes, while the total washout is strong. As a consequence, the asymmetry generated in  $N_2$  decays is completely washed out in the one-flavour approximation, while its projection on this particular flavour survives when flavour effects are taken into account. This effect, which has been first identified in the type I seesaw framework in Ref. [23], will be discussed in greater detail in Subsection 4.3. Despite the huge increase in  $Y_B$ , however, solution  $(-, -, -)$  fails to reach the WMAP level, while solution  $(+, +, -)$  is marginally successful for  $v_R \approx 10^{14}$  GeV, where  $M_2 \sim T_{in}$  (for larger values of  $v_R$ ,  $M_2 \gg T_{in}$  and  $N_2$  no longer contributes to  $Y_B$ , which then drops well below the WMAP value).

## 4.2 Relevance of the corrections to the mass relation $M_d = M_e$

The results shown in Fig. 2 were obtained assuming  $M_d = M_e$  to hold at the GUT scale, which only agrees at the order of magnitude level with the measured down quark and charged lepton masses. Let us now include the necessary corrections to this relation and investigate their effects on the final baryon asymmetry. Given the assumptions made about the Higgs sector in Section 2.3, these corrections must come from non-renormalizable operators<sup>12</sup>. The simplest possibility is to add the following terms to the superpotential (see e.g. Ref. [69]):

$$\frac{\kappa_{ij}}{\Lambda} \mathbf{16}_i \mathbf{16}_j \mathbf{10}_1 \mathbf{45} , \quad (54)$$

where we assume that the  $Y = +1$  Higgs doublet in  $\mathbf{10}_1$  does not acquire a vev, so that the mass relation  $M_D = M_u$  is left untouched<sup>13</sup>. The operators (54) will modify the reconstructed couplings  $f_{ij}$  (hence the right-handed neutrino masses and couplings) by introducing a mismatch  $U_m$  between the bases of left-handed charged lepton and down quark mass eigenstates:

$$M_e^\dagger M_e = \hat{M}_e^2 , \quad M_d^\dagger M_d = U_m^\dagger \hat{M}_d^2 U_m , \quad M_u^\dagger M_u = U_m^\dagger U_q^\dagger \hat{M}_u^2 U_q U_m , \quad (55)$$

where the mass matrices are written in the basis of charged lepton mass eigenstates, and  $\hat{M}_e$ ,  $\hat{M}_d$ ,  $\hat{M}_u$  are diagonal eigenvalue matrices. Note that  $M_d$  and  $M_e$  are no longer symmetric in the original basis, since they receive antisymmetric contributions from the operators in Eq. (54). The measured down quark and charged lepton masses do not determine completely the unitary matrix  $U_m$ , but constrain its mixing angles to lie in restricted ranges (see the Appendix for details). One of them can be taken to be either large ( $\theta_{12}^m \sim 1$ ) or somewhat smaller ( $\theta_{12}^m \sim 0.2 - 0.3$ ).

Fig. 3 shows the final baryon asymmetry for four representative choices of  $U_m$ . The main difference with the  $M_d = M_e$  case is that several choices for  $U_m$  lead to successful leptogenesis in the solution  $(+, -, +)$ . This is an interesting result, since this solution is special to the left-right symmetric seesaw mechanism: it does not correspond to dominance of either the type I or the type II seesaw mechanism in the light neutrino mass matrix in the large  $v_R$  limit. As for solution  $(-, -, -)$ , we were unable to find values of  $U_m$  and of the Majorana and high-energy phases allowing the final baryon asymmetry to reach the observed value. There is a general tendency for  $Y_B$  to reach larger values for intermediate values of  $v_R$  (typically  $10^{13} \text{ GeV} \lesssim v_R \lesssim 10^{14} \text{ GeV}$  for our choice  $\beta/\alpha = 0.1$ ), where type I and type II contributions partially compensate for each other in the light neutrino mass matrix.

The enhancement of  $Y_B$  observed for some choices of  $U_m$  can be explained by the influence of  $\theta_{12}^m$  on the CP asymmetries  $\epsilon_{i\alpha}$  and on the washout parameters  $\kappa_{i\alpha}$  (see the discussion at the end of the Appendix). In particular, solution  $(+, -, +)$  is found to be successful for large values of  $\theta_{12}^m$ , as in the sets 1 and 2 of the Appendix. We note in passing that a large mixing in  $U_m$  also enhances lepton flavour violation, so that processes like  $\mu \rightarrow e\gamma$  or  $\tau \rightarrow \mu\gamma$  might be close to their experimental limits (and a significant portion of the supersymmetric parameter space is already excluded). To illustrate the effect of  $U_m$  on the right-handed neutrino mass spectrum, we also plotted  $M_1$  and  $M_2$  as a function of  $v_R$  in Fig. 3. The enhancement of  $Y_B$  with respect to the  $M_d = M_e$  case in solutions  $(+, -, +)$  and  $(-, -, -)$  is correlated with, respectively, an increase of  $M_1$  by a factor of 10, and an increase of  $M_2$  by a factor of 5. One can also notice that successful leptogenesis is generally associated with right-handed neutrino masses above  $10^{10} \text{ GeV}$ , which indicates a conflict with the gravitino problem. Some of the solutions that are successful for  $T_{in} = 10^{11} \text{ GeV}$  might actually fail for  $T_{in} < 10^{10} \text{ GeV}$ , and we can already anticipate that this will be the case for solution  $(+, +, -)$ . We shall come back to this point in Section 5, where the dependence of  $Y_B$  on the reheating temperature will be discussed.

<sup>12</sup>One could alternatively relax the assumptions made in Section 2.3 and introduce a  $\mathbf{210}$  Higgs representation in order to generate vev's for the  $SU(2)_L$  doublet components of the  $\mathbf{126}$ . In this case, the  $f_{ij}$  couplings would contribute both to the left-right symmetric seesaw formula and to the down quark and charged lepton masses, which would render their reconstruction much more difficult.

<sup>13</sup>If the operators  $\mathbf{16}_i \mathbf{16}_j \mathbf{10}_2 \mathbf{45}$  were also present, they would give an antisymmetric contribution to  $M_D$  and the reconstruction procedure would no longer be applicable. We assume here that they are forbidden by some symmetry.

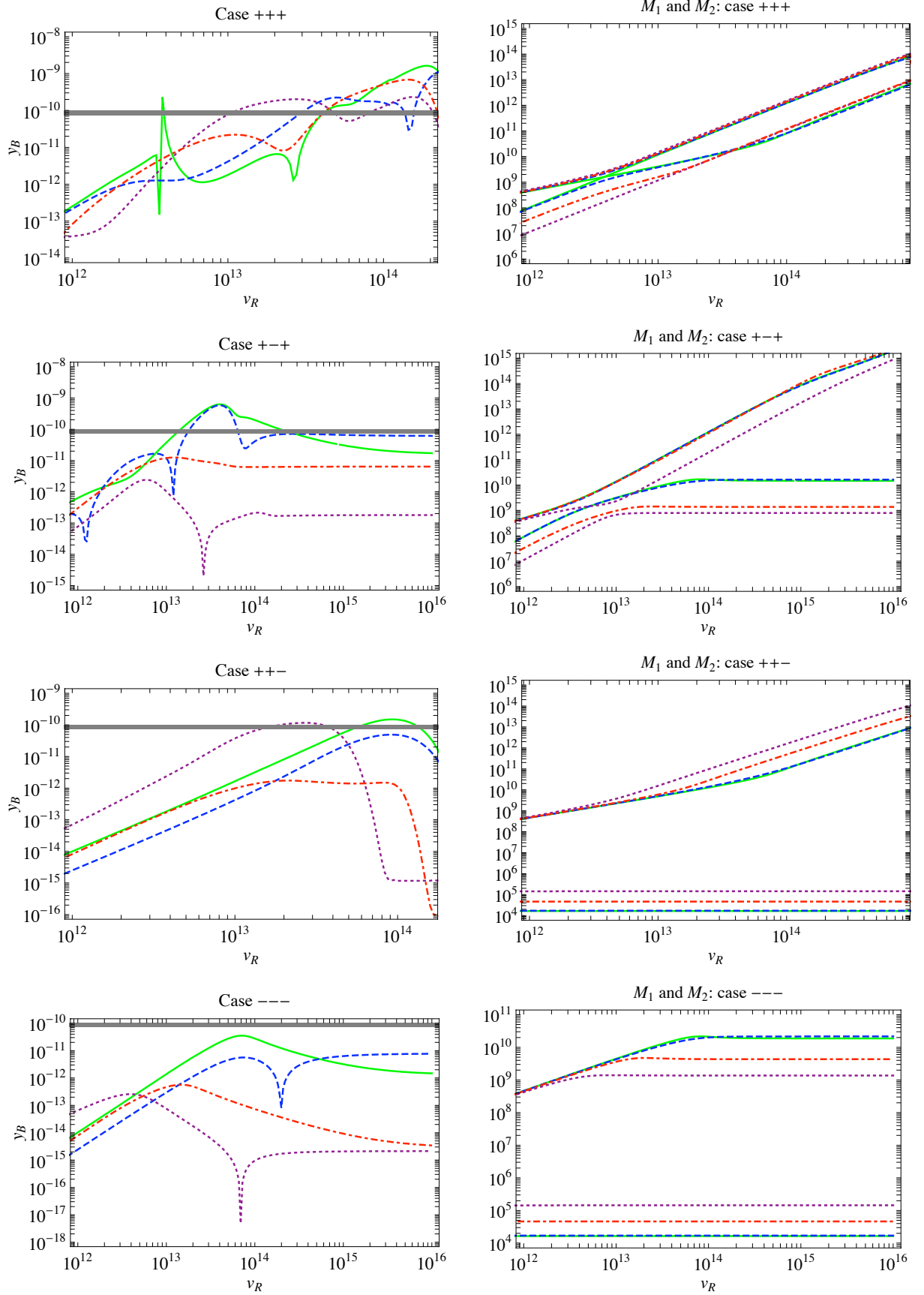


Figure 3: Final baryon asymmetry (left panels) and masses of  $N_1$  and  $N_2$  (right panels) as a function of  $v_R$  in the four reference solutions with a non-trivial  $U_m$  and a non-vanishing Majorana or high-energy phase. The solid green, dashed blue, dotted purple and dash-dotted red lines corresponds to the sets 1, 2, 3 and 4 described in the Appendix, respectively. The other input parameters are as in Fig. 2.

$(-, -, -)$	$N_{1,e}$	$N_{1,\mu}$	$N_{1,\tau}$	$N_{2,e}$	$N_{2,\mu}$	$N_{2,\tau}$
$\epsilon_{i\alpha}$	$1.1 \times 10^{-16}$	$9.6 \times 10^{-15}$	$5.8 \times 10^{-14}$	$-1.2 \times 10^{-7}$	$-6.4 \times 10^{-8}$	$-3.4 \times 10^{-7}$
$\kappa_{i\alpha}$	0.04	17.2	16.2	2.3	0.7	2.7
$(+, +, -)$	$N_{1,e}$	$N_{1,\mu}$	$N_{1,\tau}$	$N_{2,e}$	$N_{2,\mu}$	$N_{2,\tau}$
$\epsilon_{i\alpha}$	$1.2 \times 10^{-16}$	$9.7 \times 10^{-15}$	$5.7 \times 10^{-14}$	$7.0 \times 10^{-7}$	$2.0 \times 10^{-7}$	$2.6 \times 10^{-6}$
$\kappa_{i\alpha}$	0.04	17.2	16.2	0.5	0.2	3.5

Table 1: Values of  $\epsilon_{i\alpha}$  and  $\kappa_{i\alpha}$  ( $i = 1, 2$ ;  $\alpha = e, \mu, \tau$ ) in solutions  $(-, -, -)$  and  $(+, +, -)$ . The input parameters are chosen as in Fig. 2, and the  $B - L$  breaking scale is  $v_R = 10^{14}$  GeV.

### 4.3 Flavour effects and $N_2$ leptogenesis

Let us now discuss in more quantitative terms the interplay of flavour effects and  $N_2$  decays in the four solutions  $(\pm, \pm', -)$ , which are characterized by a strong hierarchy between the masses of the two lightest right-handed neutrinos. As mentioned above, the lepton asymmetry generated by  $N_2$  is exponentially washed out by  $N_1$ -related processes in the one-flavour approximation. Since  $N_1$  has a small coupling to a particular lepton flavour, however, the asymmetry in this flavour is only mildly washed out in the flavour-dependent treatment, and this explains the spectacular enhancement of  $Y_B$  observed in Fig. 2. We shall refer to this situation as “flavour-dependent  $N_2$  leptogenesis” in the following.

For flavour-dependent  $N_2$  leptogenesis to be possible, some conditions on the CP asymmetries and washout parameters must be satisfied. In Table 1, we list the values of  $\epsilon_{i\alpha}$  and  $\kappa_{i\alpha}$  ( $i = 1, 2$ ;  $\alpha = e, \mu, \tau$ ) in the  $(-, -, -)$  and  $(+, +, -)$  solutions for  $v_R = 10^{14}$  GeV, assuming the same input parameters as in Fig. 2 (in particular,  $U_m = \mathbb{1}$ ,  $\Phi_2^y = \pi/4$  and all other CP-violating phases are set to zero). Both solutions exhibit a similar pattern of flavoured parameters: the CP asymmetries in  $N_1$  decays are extremely small ( $\epsilon_{1\alpha} < 10^{-13}$ ), and the washout induced by  $N_1$  is strong except for the electron flavour ( $\kappa_{1e} = 0.04$ , while  $\kappa_{1\mu} \approx \kappa_{1\tau} \approx 16$ ). By contrast, the CP asymmetries in  $N_2$  decays are in the  $(10^{-7} - 10^{-6})$  range, and the  $N_2$ -induced washout is moderate.

Let us see in detail how these features explain the results observed in Fig. 2, focusing on solution  $(+, +, -)$  for definiteness (for earlier discussions of flavour-dependent  $N_2$  leptogenesis in the type I seesaw framework, see Refs. [23] and [52]).  $N_2$  decays first generate asymmetries  $(Y_{\Delta_\alpha})_{N_2}$  in all three lepton flavours. Since  $M_1 \ll M_2$ , the processes involving  $N_1$  are out of equilibrium at  $\bar{T} \sim M_2$ , and the  $(Y_{\Delta_\alpha})_{N_2}$  can be computed taking into account  $N_2$ -induced washout only. Neglecting off-diagonal entries in the  $A$  matrix, one obtains:

$$(Y_{\Delta_e})_{N_2} \simeq -4 \times 10^{-10}, \quad (Y_{\Delta_\mu})_{N_2} \simeq -4 \times 10^{-11}, \quad (Y_{\Delta_\tau})_{N_2} \simeq -10^{-9}, \quad (56)$$

while in the one-flavour approximation the  $B - L$  asymmetry induced by  $N_2$  is  $(Y_{B-L}^{1FA})_{N_2} \simeq -6 \times 10^{-10}$ . As the Universe cools down,  $N_1$ -related washout processes come into equilibrium, and the evolution of the  $Y_{\Delta_\alpha}$ 's is then governed by the following Boltzmann equations:

$$Y'_{\Delta_\alpha}(z) = 2\kappa_{1\alpha} A_{\alpha\alpha} W_1(z) Y_{\Delta_\alpha}(z) + 2\kappa_{1\alpha} \sum_{\beta \neq \alpha} A_{\alpha\beta} W_1(z) Y_{\Delta_\beta}(z), \quad (57)$$

in which the source term proportional to  $\epsilon_{1\alpha}$  has been neglected because of its smallness. Eq. (57) yields the formal solution:

$$Y_{\Delta_\alpha}(z) \simeq (Y_{\Delta_\alpha})_{N_2} e^{2A_{\alpha\alpha}\kappa_{1\alpha} \int_{zin}^z dx W_1(x)} + 2\kappa_{1\alpha} \sum_{\beta \neq \alpha} A_{\alpha\beta} \int_{zin}^z dx W_1(x) Y_{\Delta_\beta}(x) e^{2A_{\alpha\alpha}\kappa_{1\alpha} \int_x^z dy W_1(y)}, \quad (58)$$

where the first term corresponds to the depletion of  $Y_{\Delta_\alpha}$  due to  $N_1$ -related washout processes, whereas the second term represents the effect of the flavour mixing induced by the off-diagonal entries in the  $A$

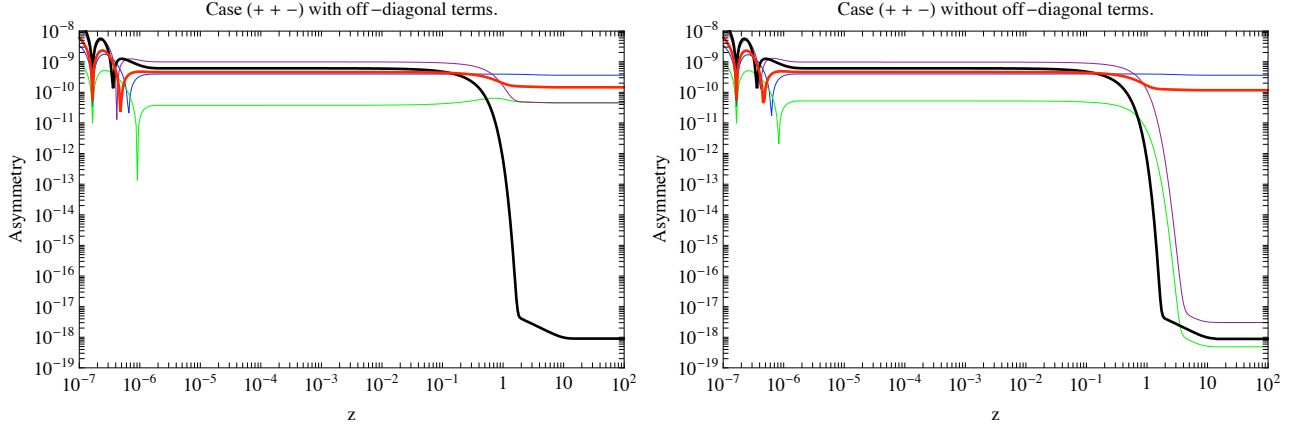


Figure 4: Evolution of the asymmetries as a function of  $z = M_1/T$  in the  $(+, +, -)$  solution, with the off-diagonal entries of the  $A$  matrix included (left panel) and omitted (right panel). The thin lines represent the three lepton flavour asymmetries:  $Y_{\Delta_e}$  in blue (medium grey),  $Y_{\Delta_\mu}$  in green (light grey),  $Y_{\Delta_\tau}$  in purple (dark grey), while the thick red (medium grey) and black lines stand for  $Y_B$  and  $Y_{B-L}^{1FA}$ , respectively. The input parameters are chosen as in Fig. 2, and the  $B - L$  breaking scale is  $v_R = 10^{14}$  GeV.

matrix. Neglecting the off-diagonal entries of the  $A$  matrix for the moment, and omitting for simplicity the scattering terms in  $W_1(z)$ , one obtains:

$$Y_{\Delta_\alpha}^d \simeq e^{\frac{3\pi}{4} A_{\alpha\alpha} \kappa_{1\alpha}} (Y_{\Delta_\alpha})_{N_2}, \quad (59)$$

where we have used  $\int_0^\infty dz z^3 K_1(z) = 3\pi/2$ . Since  $\kappa_{1e} \ll 1 \ll \kappa_{1\mu(\tau)}$ , the asymmetry in the electron flavour is almost unaffected by  $N_1$ -induced washout, while  $(Y_{\Delta_\mu})_{N_2}$  and  $(Y_{\Delta_\tau})_{N_2}$  are exponentially diluted, namely by a factor of order  $10^{-11}$ . The final baryon asymmetry is<sup>14</sup>:

$$Y_B \simeq \frac{10}{31} Y_{\Delta_e}^d \simeq \frac{10}{31} 0.92 (Y_{\Delta_e})_{N_2} \simeq -1.2 \times 10^{-10}, \quad (60)$$

in good agreement with the numerical result. In the one-flavour approximation instead, the  $B - L$  asymmetry generated in  $N_2$  decays is completely washed out by  $N_1$ -related processes:

$$Y_{B-L}^{1FA} \simeq e^{-\frac{3\pi}{4} \kappa_1} (Y_{B-L}^{1FA})_{N_2} \simeq 6 \times 10^{-35} (Y_{B-L}^{1FA})_{N_2}, \quad (61)$$

so that the dominant contribution to  $Y_{B-L}^{1FA}$  actually comes from  $N_1$  decays, in spite of the smallness of  $\epsilon_1$  (an analogous statement can be made about  $Y_{\Delta_\mu}$  and  $Y_{\Delta_\tau}$  in the flavour-dependent treatment). All these results are illustrated in the right panel of Fig. 4.

Let us now add the effect of the off-diagonal entries in the  $A$  matrix. The contribution to  $Y_{\Delta_\alpha}$  of the second term in the right-hand side of Eq. (57) has been evaluated in Ref. [51], in the non-supersymmetric case:

$$Y_{\Delta_\alpha}^{od} \simeq \frac{1.3 \kappa_{1\alpha}}{1 + 0.8(-A_{\alpha\alpha} \kappa_{1\alpha})^{1.17}} \sum_{\beta \neq \alpha} A_{\alpha\beta} Y_{\Delta_\beta}^d. \quad (62)$$

This flavour mixing does not affect  $Y_{\Delta_e}$ , but prevents the complete depletion of  $Y_{\Delta_\mu}$  and  $Y_{\Delta_\tau}$ :

$$Y_{\Delta_{\mu(\tau)}}^{od} \simeq 0.12 Y_{\Delta_e}^d \simeq -4.4 \times 10^{-11}. \quad (63)$$

The final baryon asymmetry is only marginally affected, reaching  $Y_B \simeq -1.5 \times 10^{-10}$ . These analytic estimates are confirmed by the numerical results shown in the left panel of Fig. 4.

<sup>14</sup>As explained earlier in this section, the sign of  $Y_B$  is not relevant since it can be reverted by changing the sign of  $\Phi_2^u$  (if one neglects the small contribution of  $\delta_{CKM}$  to  $Y_B$ ).

We conclude that flavour effects play a crucial role in the four solutions  $(\pm, \pm', -)$ , where they render  $N_2$  leptogenesis possible. In spite of the spectacular enhancement of the final baryon asymmetry with respect to the one-flavour approximation, however, successful flavour-dependent  $N_2$  leptogenesis is difficult to achieve, as shown by Figs. 2 and 3. This is even more so in solution  $(-, -, -)$ , which in the large  $v_R$  limit reduces to the type I seesaw case, in which flavour-dependent  $N_2$  leptogenesis was originally proposed as a way to achieve successful baryogenesis in GUTs [23].

## 5 Dependence on the input parameters

The results presented in the previous section were obtained for fixed values of the light neutrino parameters: we assumed a normal mass hierarchy with  $m_1 = 10^{-3}$  eV,  $\theta_{13} = 0$  and no CP violation in the PMNS mixing matrix, while the oscillation parameters were taken from Ref. [37]. Furthermore, the relation  $M_D = M_u$  was assumed and the Boltzmann equations were evolved from  $T_{in} = 10^{11}$  GeV. In this section, we numerically study the influence of these input parameters on the final baryon asymmetry.

### 5.1 Dependence on the light neutrino parameters

Let us first study the impact of the yet unmeasured light neutrino parameters: the lightest neutrino mass, the mixing angle  $\theta_{13}$  and the Dirac phase  $\delta_{PMNS}$ , and finally the type of mass hierarchy.

#### 5.1.1 Lightest neutrino mass (normal mass hierarchy)

Since the flavour-dependent CP asymmetries  $\epsilon_{1\alpha}$  are bounded by (note that the upper bound is the same as in the type I case [43]):

$$|\epsilon_{1\alpha}| \leq \epsilon_{1\alpha}^{max} \equiv \frac{3}{8\pi} \frac{M_1 m_{max}}{v_u^2} \sqrt{\frac{\kappa_{1\alpha}}{\kappa_1}}, \quad (64)$$

and the type I inequality  $\kappa_1 \geq m_1/m_\star$  does not hold, one may expect that successful leptogenesis is easier to achieve for quasi-degenerate light neutrinos,  $m_1 \gtrsim 0.1$  eV. However, varying  $m_1$  also modifies the reconstructed right-handed neutrino parameters, which in turn affects the CP asymmetries and washout parameters. In particular, the right-handed neutrino masses are modified by an increase of  $m_1$  in the following way (the right-handed neutrino couplings  $\lambda_{i\alpha}$  are also affected via the  $U_f$  matrix): the  $M_i$ 's belonging to a ‘‘type I branch’’ decrease, while the ones belonging to a ‘‘type II branch’’ rise. This behaviour can be understood by noticing that, to a good approximation, the right-handed neutrino masses are proportional to the  $x_i$ 's (see the Appendix B of Ref. [29]). Since raising  $m_1$  increases the value of the  $z_i$ 's, Eq. (12) implies that the  $M_i$  associated with some  $x_j^-$  (‘‘type I branch’’) decreases, while the  $M_i$  associated with some  $x_j^+$  (‘‘type II branch’’) shows the opposite behaviour<sup>15</sup>. These considerations explain to a large extent the impact of a variation of  $m_1$  on the final baryon asymmetry, since the upper bound on  $\epsilon_{1\alpha}$  is proportional to  $M_1$  and  $\kappa_{1\alpha} \propto 1/M_1$ : an increase in  $M_1$  tends to enhance the CP asymmetry in  $N_1$  decays and to reduce the  $N_1$  washout parameters. An analogous statement can be made about  $M_2$  and the  $N_2$ -related leptogenesis parameters.

Fig. 5 shows the region of the  $(m_1, v_R)$  parameter space where  $|Y_B| > Y_B^{WMAP}$  for solutions  $(+, +, +)$ ,  $(+, -, +)$  and  $(+, +, -)$ , and where  $|Y_B| > 0.1 Y_B^{WMAP}$  for solution  $(-, -, -)$ , which fails to generate the observed baryon asymmetry. The choice for  $U_m$  and the high-energy phases corresponds to the set 1 described in the Appendix, the other input parameters being fixed as in Fig. 2. In the  $(+, +, +)$  case, increasing  $m_1$  amounts to shift the range of  $v_R$  for which leptogenesis is successful towards lower values. This is consistent with the fact that  $M_1$  and  $M_2$  grow with  $m_1$ , and that the thermal production

<sup>15</sup>Strictly speaking, this is only true for  $4\alpha\beta \ll |z_j|^2$  ( $v_R \gg 2\sigma_u v_u^4/M_\Delta |z_j|^2$ ). In the opposite limit (which is not relevant for the discussion below),  $x_j$  is almost independent of  $z_j$  and the associated  $M_i$  is not affected by an increase of  $m_1$ .

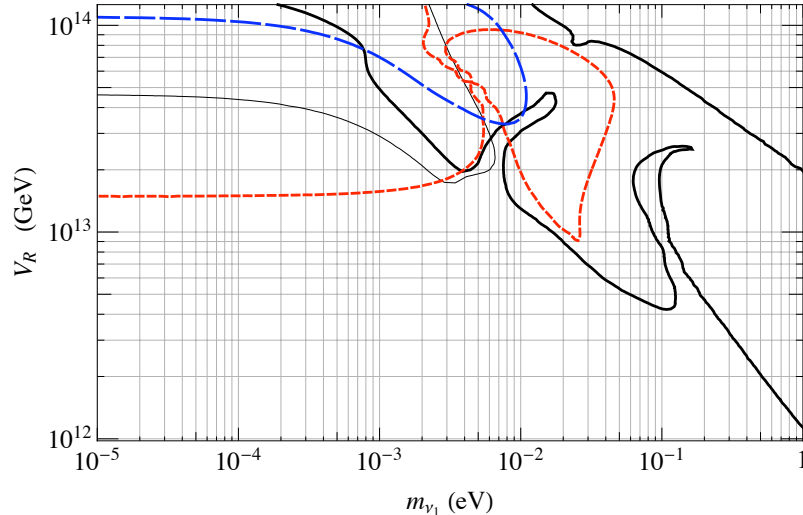


Figure 5: Regions of the  $(m_1, v_R)$  parameter space where  $|Y_B| > Y_B^{WMAP}$  for solutions  $(+, +, +)$ ,  $(+, -, +)$  and  $(+, +, -)$ , and where  $|Y_B| > 0.1 Y_B^{WMAP}$  for solution  $(-, -, -)$ . These regions are delimited by the thick black contour in the  $(+, +, +)$  case, the dashed red contour for  $(+, -, +)$ , the long-dashed blue contour for  $(+, +, -)$ , and the thin black contour for  $(-, -, -)$ . Inputs: set 1 of the Appendix for  $U_m$  and the high-energy phases; other input parameters as in Fig. 2.

of  $N_i$  is Boltzmann-suppressed for  $M_i > T_{in}$ . The behaviour of the other solutions is more interesting: in all three cases, the final baryon asymmetry is suppressed for a quasi-degenerate light neutrino mass spectrum. In the two solutions in which  $N_2$  leptogenesis plays a crucial role, namely  $(+, +, -)$  and  $(-, -, -)$ , this is due to the fact that the  $N_1$ -induced washout becomes strong for all flavours, as a result of the decrease of  $M_1$  (also, for  $(-, -, -)$ ,  $M_2$  decreases with growing  $m_1$ ). In the  $(+, -, +)$  case, a larger  $m_1$  implies a smaller  $M_1$  and thus reduces the final baryon asymmetry. As a result, leptogenesis fails for a quasi-degenerate light neutrino mass spectrum in all reference solutions but  $(+, +, +)$ . For the input parameters used in Fig. 5, successful leptogenesis requires  $m_1 \lesssim 0.01$  eV for solution  $(+, +, -)$ , and  $m_1 \lesssim 0.05$  eV for solution  $(+, -, +)$ .

### 5.1.2 $\theta_{13}$ and $\delta_{PMNS}$

We now turn to the dependence of the final baryon asymmetry on  $\theta_{13}$  and  $\delta_{PMNS}$ , the two unknown light neutrino parameters which control the amount of CP violation in oscillations. In Fig. 6, we first show the effect of varying  $\theta_{13}$  alone, from our reference value  $\theta_{13} = 0^\circ$  to the experimental upper limit  $\theta_{13} = 13^\circ$ , assuming  $\delta_{PMNS} = 0$ . The choice for  $U_m$  and the high-energy phases corresponds to the set 1 of the Appendix. Furthermore, the Boltzmann equations are evolved from a somewhat lower initial temperature than in the previous plots:  $T_{in} = 7 \times 10^9$  GeV for  $(+, +, +)$  and  $(+, -, +)$ , and  $T_{in} = 5 \times 10^{10}$  GeV for  $(+, +, -)$  and  $(-, -, -)$ . The other input parameters are chosen as in Fig. 2. As can be seen from Fig. 6, increasing  $\theta_{13}$  generally reduces the final baryon asymmetry, especially in solutions  $(\pm, \pm, -)$  where the effect is particularly pronounced. Solution  $(+, +, +)$  behaves differently, although in this case too the maximum value of  $Y_B$  is obtained for small values of  $\theta_{13}$ .

One could be tempted to conclude from Fig. 6 that (at least for the chosen input parameters) successful leptogenesis favours small values of  $\theta_{13}$ . However, it is not legitimate to impose  $\delta_{PMNS} = 0$ : since  $\theta_{13}$  and  $\delta_{PMNS}$  always appear in combination in  $U_{PMNS}$ , one should study their joint effect on the final baryon asymmetry. This is done in Fig. 7, for the same choice of input parameters as in Fig. 6, but for a fixed value of the  $B - L$  breaking scale  $v_R$ . One can see that successful leptogenesis is compatible with a “large” value of  $\theta_{13}$  ( $\theta_{13} \gtrsim 5^\circ$ ) as soon as  $\delta_{PMNS}$  is allowed to be different from zero. Such values

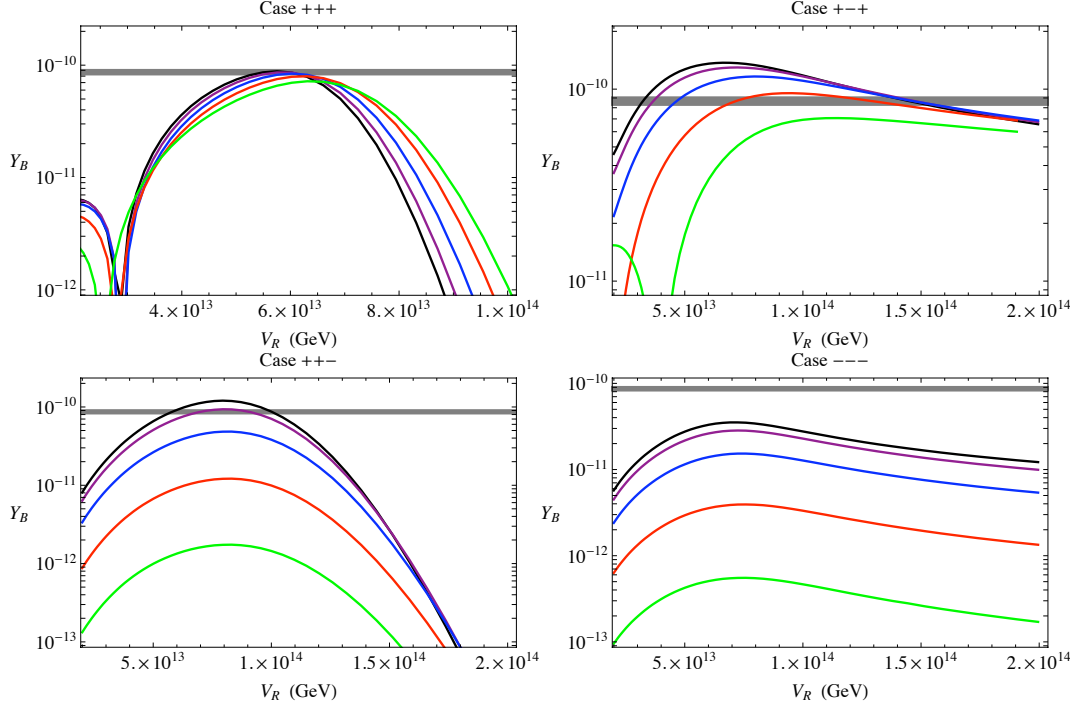


Figure 6: The final baryon asymmetry as a function of  $v_R$  in the four reference solutions, for  $\delta_{PMNS} = 0$  and different values of  $\theta_{13}$ :  $\theta_{13} = 0^\circ$  (black),  $2^\circ$  (purple),  $5^\circ$  (blue),  $9^\circ$  (red) and  $13^\circ$  (green / light grey). Inputs: set 1 of the Appendix for  $U_m$  and the high-energy phases;  $T_{in} = 7 \times 10^9$  GeV for  $(+, +, +)$  and  $(+, -, +)$ , while  $T_{in} = 5 \times 10^{10}$  GeV for  $(+, +, -)$  and  $(-, -, -)$ ; other input parameters as in Fig. 2.

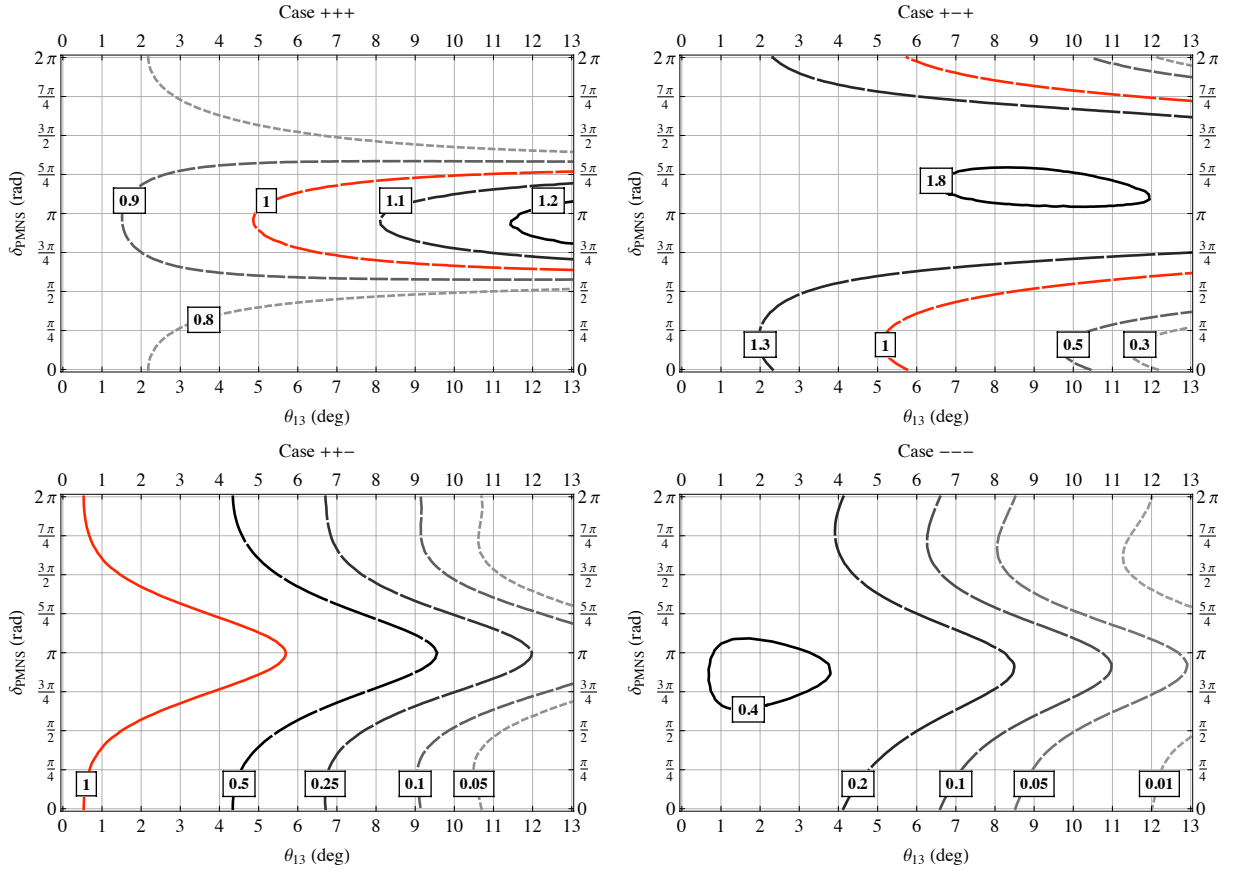


Figure 7: Contour lines of the ratio  $|Y_B|/Y_B^{WMAP}$  in the four reference solutions, as a function of  $\theta_{13}$  and  $\delta_{PMNS}$ . The input parameters are the same as in Fig. 6, and the  $B-L$  breaking scale has been fixed at  $v_R = 5 \times 10^{13}$  GeV for  $(+, +, +)$  and  $(+, -, +)$ , and at  $v_R = 6 \times 10^{13}$  GeV for  $(+, +, -)$  and  $(-, -, -)$ .

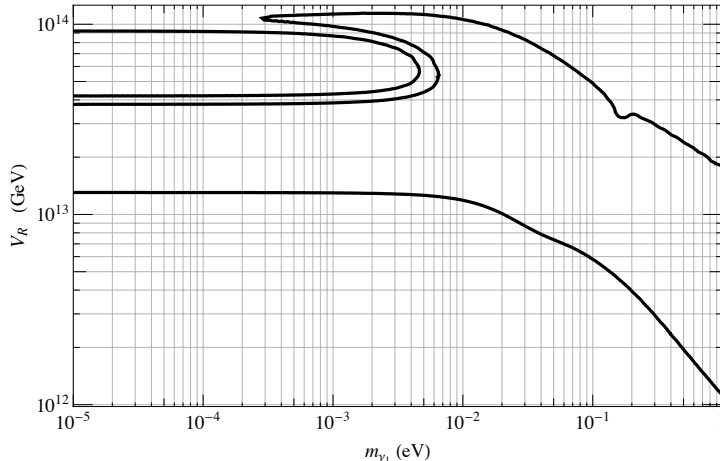


Figure 8: Region of the  $(m_3, v_R)$  parameter space where  $|Y_B| > Y_B^{WMAP}$  in the  $(+, +, +)$  solution, assuming an inverted light neutrino mass hierarchy (delimited by the black contour). Inputs: set 1 of the Appendix for  $U_m$  and the high-energy phases; other input parameters as in Fig. 2.

of  $\theta_{13}$  are within the reach of upcoming reactor and first generation superbeam experiments (for a brief review, see e.g. Ref. [70]). For instance,  $\theta_{13}$  just below the present experimental limit together with  $\delta_{PMNS} \approx 5\pi/8$  is compatible with  $Y_B = Y_B^{WMAP}$  both in the  $(+, +, +)$  and in the  $(+, -, +)$  solution. Although Fig. 7 was obtained for a specific set of input parameters, we can conclude that successful leptogenesis is possible for values of  $\theta_{13}$  and  $\delta_{PMNS}$  such that CP violation in the leptonic sector can be established in future neutrino superbeam experiments.

### 5.1.3 Inverted mass hierarchy

Assuming an inverted light neutrino mass hierarchy leads to significantly different results from the normal hierarchy case, although the gross qualitative features are preserved (in particular, solution  $(+, +, +)$  generally leads to successful leptogenesis, while for solution  $(+, -, +)$  this depends on the choice of  $U_m$  and of the Majorana and high-energy phases). In this paper, we do not attempt to perform a general study of the inverted hierarchy case, which has already been investigated in Ref. [30], in the one-flavour approximation and assuming  $M_d = M_e$ . To illustrate some of the differences with the normal hierarchy case, we just display in Fig. 8 the plot analogous to the one in Fig. 5. Only solution  $(+, +, +)$  is represented there, since for the choice of input parameters made in Fig. 5 none of the other reference solutions leads to successful leptogenesis in the inverted hierarchy case. This is already a noticeable difference with the normal hierarchy case. As far as solution  $(+, +, +)$  is concerned, some differences with respect to the normal hierarchy case can be seen in the region where the lightest neutrino mass lies below a few  $10^{-3}$  eV. We were not able to reproduce the result of Ref. [30], which finds that solution  $(+, -, +)$  can generate the observed baryon asymmetry in the absence of corrections to the mass relation  $M_d = M_e$ , in the region where  $M_1 \approx M_2$ . This may be due to the differences in the treatment of leptogenesis: the study of Ref. [30] was performed in the one-flavour approximation, assuming initial thermal abundances for the right-handed neutrinos, while we solved the flavour-dependent Boltzmann equations with  $T_{in} = 10^{11}$  GeV and vanishing initial abundances. Furthermore, Ref. [30] used the non-supersymmetric analogue of Eq. (32) in the computation of the CP asymmetry, while we used Eq. (34), which reproduces the correct behaviour of the self-energy contribution in the limit of exactly degenerate right-handed neutrinos.

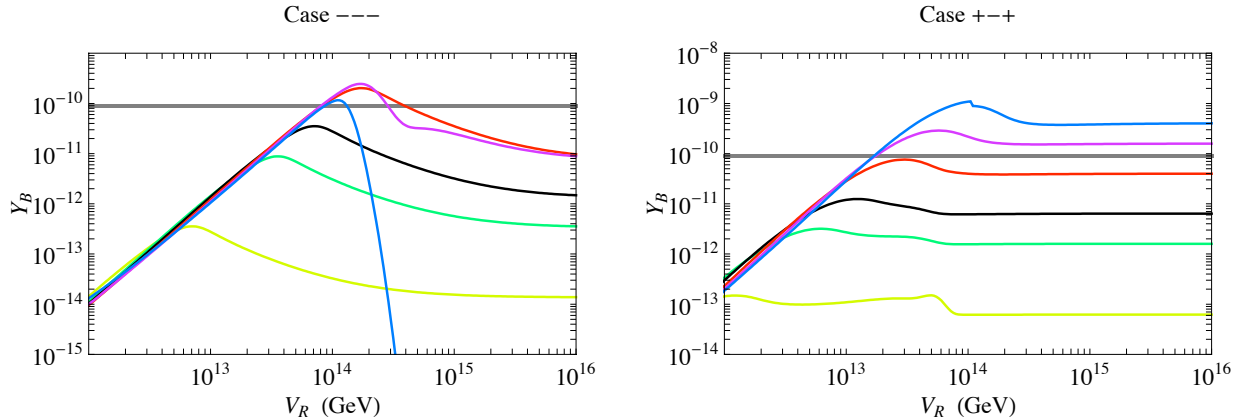


Figure 9: The final baryon asymmetry as a function of  $v_R$  for different values of  $y_2$ , from  $y_2/y_c(M_{GUT}) = 0.1$  (yellow/light grey) to  $y_2/y_c(M_{GUT}) = 10$  (blue/dark grey). The reference case  $y_2 = y_c$  is plotted in black. Left panel: solution  $(-, -, -)$ , set 1 for  $U_m$  and the high-energy phases; right panel: solution  $(+, -, +)$ , set 4 for  $U_m$  and the high-energy phases. The other input parameters are as in Fig. 2.

## 5.2 Impact of corrections to the mass relation $M_D = M_u$

In the preceding subsections, we studied the dependence of the final baryon asymmetry on the values of the yet unmeasured light neutrino parameters. Let us now turn to the influence of the high-energy Dirac couplings. So far we assumed that the mass relation  $M_D = M_u$  holds at the GUT scale, while  $M_d = M_e$  receives corrections from non-renormalizable operators. In this subsection, we study the effect of a departure from  $M_D = M_u$ . More specifically, we assume that  $M_D$  and  $M_u$  are still diagonal in the same basis<sup>16</sup> but that their eigenvalues differ ( $y_i \neq y_{u_i}$ ). This has a direct impact on the right-handed neutrino mass spectrum, since the  $M_i$  associated with some  $x_j^-$  is to a good approximation proportional to  $y_j^2$  in the regime  $v_R \gg 2\sigma_u v_u^4/M_\Delta |z_j|^2$ , while the  $M_i$  associated with some  $x_j^+$  is independent of  $y_j$  (see the Appendix B of Ref. [29]). In particular, one has  $M_1 \propto y_2^2$  in solution  $(+, -, +)$  and  $M_2 \propto y_2^2$  in solution  $(-, -, -)$ . One thus expects that raising  $y_2$  will enhance the final baryon asymmetry by increasing the  $\epsilon_{1\alpha}$ 's in the former case, and the  $\epsilon_{2\alpha}$ 's in the latter case.

This is shown in Fig. 9, in which  $(y_2/y_c)(M_{GUT})$  is varied between 0.1 and 10 in solutions  $(+, -, +)$  (right panel) and  $(-, -, -)$  (left panel). We can see that the final baryon asymmetry increases with growing  $y_2$  in both solutions. In particular, successful leptogenesis becomes possible in the  $(-, -, -)$  case for large enough  $y_2$  (for  $y_2 = 10 y_c$ , however,  $N_2$  becomes too heavy to be thermally produced above  $v_R \sim 10^{14}$  GeV, which results in the Boltzmann suppression of  $Y_B$ ). This conclusion is however dependent on the input  $T_{in} = 10^{11}$  GeV: it does not hold for the more realistic choice  $T_{in} = 10^{10}$  GeV (see the discussion in the next subsection about the gravitino problem). In the  $(+, -, +)$  case, successful leptogenesis is possible for values of  $v_R$  as large as a few  $10^{16}$  GeV, and this conclusion also holds for  $T_{in} = 10^{10}$  GeV. This is an interesting result, since gauge coupling unification favours a one-step breaking of the  $SO(10)$  symmetry, with a  $B - L$  breaking scale close to the GUT scale (a lower  $B - L$  breaking scale is however not excluded [71]). Fig. 9 also shows that  $y_2 > y_c$  allows solution  $(+, -, +)$  to be successful with a  $U_m$  containing only small mixing angles (set 4), thus alleviating the constraints on the superpartner spectrum coming from the non-observation of lepton flavour violating processes such as  $\mu \rightarrow e\gamma$ .

<sup>16</sup>This is a natural assumption if the CKM matrix mainly comes from the down quark sector. In this case, and in the absence of cancellations between the different contributions to  $M_D$  and  $M_u$ , both matrices have a strong hierarchical structure with mixing angles smaller than the CKM angles. The relative rotation between the bases in which  $M_D$  and  $M_u$  are diagonal can then be neglected in the reconstruction procedure.

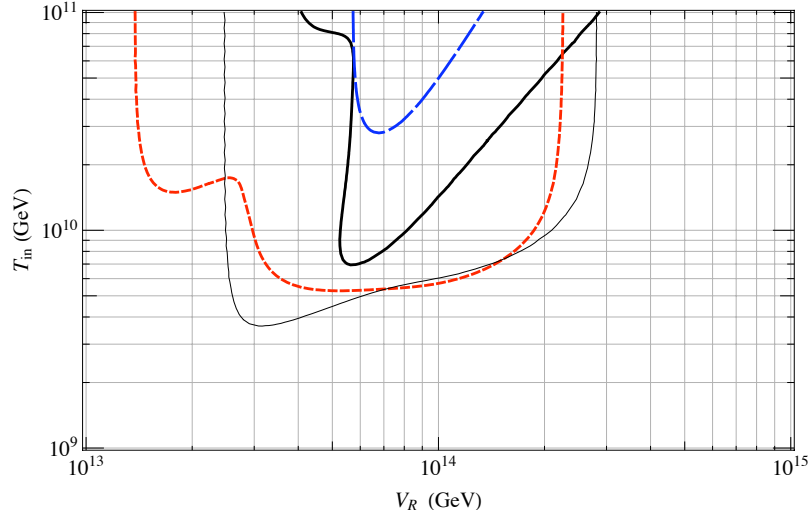


Figure 10: Regions of the  $(v_R, T_{in})$  parameter space where  $|Y_B| > Y_B^{WMAP}$  for solutions  $(+, +, +)$ ,  $(+, -, +)$  and  $(+, +, -)$ , and where  $|Y_B| > 0.1 Y_B^{WMAP}$  for solution  $(-, -, -)$ . These regions are delimited by the thick black contour in the  $(+, +, +)$  case, the dashed red contour for  $(+, -, +)$ , the long-dashed blue contour for  $(+, +, -)$ , and the thin black contour for  $(-, -, -)$ . Inputs: set 1 of the Appendix for  $U_m$  and the high-energy phases; other input parameters as in Fig. 2.

### 5.3 Dependence on the reheating temperature

The numerical results presented so far were obtained starting the evolution of the Boltzmann equations at  $T_{in} = 10^{11}$  GeV, in the approximation where the dynamics of reheating is neglected. In this approach,  $T_{in}$  can be identified with the reheating temperature. In order to estimate how severe the tension between successful leptogenesis and the gravitino problem is, we therefore proceed to study the dependence of the final baryon asymmetry on  $T_{in}$ . Fig. 10 shows the regions of the  $(v_R, T_{in})$  parameter space where  $|Y_B| > Y_B^{WMAP}$  for solutions  $(+, +, +)$ ,  $(+, -, +)$  and  $(+, +, -)$ , and where  $|Y_B| > 0.1 Y_B^{WMAP}$  for solution  $(-, -, -)$ . The choice for  $U_m$  and the high-energy phases corresponds to the set 1 of the Appendix, the other input parameters being fixed as in Fig. 2. One can see that solution  $(+, -, +)$  succeeds in generating the observed baryon asymmetry for values of  $T_{in}$  as low as  $5 \times 10^9$  GeV, whereas solutions  $(+, +, +)$  and  $(+, +, -)$  require  $T_{in} \gtrsim 7 \times 10^9$  GeV and  $T_{in} \gtrsim 3 \times 10^{10}$  GeV, respectively. While these numbers have been obtained for a particular choice of the input parameters, they unambiguously show that successful leptogenesis can be achieved with a reheating temperature below  $10^{10}$  GeV in solutions  $(+, +, +)$  and  $(+, -, +)$ . As for solution  $(+, +, -)$ ,  $T_{in} > 10^{10}$  GeV was found to be a necessary condition for successful leptogenesis for all sets of input parameters we considered. This allows us to conclude that, for generic input parameters, the solution  $(+, +, -)$  fails to generate the observed baryon asymmetry if the reheating temperature is lower than  $10^{10}$  GeV.

As discussed at the end of Section 3, there are strong constraints on the reheating temperature from gravitino cosmology, and this potentially conflicts with successful thermal leptogenesis. Nevertheless, some supersymmetric scenarios can accommodate a reheating temperature in the  $(10^9 - 10^{10})$  GeV range, as required for solutions  $(+, +, +)$  and  $(+, -, +)$  to generate the correct amount of baryon asymmetry. One possibility is that the gravitino is the LSP; the constraint that its relic density does not exceed the dark matter abundance reads  $T_{RH} \lesssim (10^9 - 10^{10})$  GeV for  $m_{3/2} \sim 100$  GeV [39]. This scenario is further constrained by the requirement that the NLSP decays do not alter the success of Big Bang nucleosynthesis (BBN), which can be satisfied e.g. by a sneutrino NLSP [72] or by assuming some amount of  $R$ -parity violation [73]. Another way of avoiding the strong constraints on the reheating temperature is to assume an extremely light gravitino [74],  $m_{3/2} \leq 16$  eV [75] (where the upper bound comes from WMAP and Lyman- $\alpha$  forest data), or a very heavy gravitino [76],  $m_{3/2} \gtrsim 50$  TeV. In

the former case, the gravitino decouples when it is still relativistic and escapes the overproduction problem, while the NLSP is sufficiently short-lived to decay before BBN. In the latter case, the gravitino decays before nucleosynthesis and does not affect the light element abundances; furthermore, the LSPs produced in its decays are within the observed dark matter abundance for  $T_{RH} \lesssim 10^{10}$  GeV [77].

## 6 Conclusions

In this paper, we studied thermal leptogenesis in a broad class of supersymmetric  $SO(10)$  models with a left-right symmetric seesaw mechanism, including flavour effects and the contribution of the next-to-lightest right-handed neutrino supermultiplet. Assuming  $M_D = M_u$  and a normal hierarchy of light neutrino masses, we found that successful leptogenesis is possible with a reheating temperature in the  $(10^9 - 10^{10})$  GeV range for 4 out of the 8 reconstructed right-handed neutrino mass spectra<sup>17</sup>, corresponding to solutions  $(\pm, +, +)$  and  $(\pm, -, +)$ . In the remaining 4 solutions, leptogenesis is dominated by  $N_2$  decays, as in the type I seesaw case; among those, solutions  $(\pm, +, -)$  succeed in generating the observed baryon asymmetry for reheating temperatures above  $10^{10}$  GeV. These results show that  $SO(10)$  models in which the Dirac mass matrix and the up quark mass matrix have a similar hierarchical structure are compatible with successful thermal leptogenesis if the seesaw mechanism is of the left-right symmetric type. As a byproduct, we found that solution  $(-, -, -)$ , which mimics the type I seesaw in the large  $v_R$  limit, fails to generate the right amount of baryon asymmetry in this limit. This suggests that successful flavour-dependent  $N_2$  leptogenesis in  $SO(10)$  models with a type I seesaw mechanism requires large corrections to the mass formula  $M_D = M_u$ , especially if one insists on  $T_{RH} < 10^{10}$  GeV.

Both flavour effects and the corrections to the mass relation  $M_d = M_e$  were found to be crucial ingredients for the success of solutions  $(\pm, -, +)$  and, for  $T_{RH} > 10^{10}$  GeV, of solutions  $(\pm, +, -)$ . In the former case, flavour effects increase the final baryon asymmetry by up to one order of magnitude, while in the latter case they allow a particular lepton flavour asymmetry generated in  $N_2$  decays to survive the washout by  $N_1$ -related processes, resulting in a spectacular enhancement of the final baryon asymmetry with respect to the one-flavour approximation. We also studied the dependence of the results on the unknown light neutrino parameters ( $\theta_{13}$ ,  $\delta_{PMNS}$  and the type of mass hierarchy), as well as on corrections to the mass relation  $M_D = M_u$  and on the reheating temperature. Moderate deviations from  $M_D = M_u$  were shown to extend the region of parameter space in which leptogenesis is successful; in particular, solution  $(+, -, +)$  was found to be successful for values of the  $B - L$  breaking scale as large as  $10^{16}$  GeV, as preferred by supersymmetric gauge coupling unification.

We believe that the results presented in this paper (which extend and put on a more solid basis the ones of Refs. [29, 30]) make  $SO(10)$  models in which neutrino masses originate from the left-right symmetric seesaw mechanism more attractive. Other aspects of the phenomenology of these models, such as lepton flavour violation (which was briefly discussed in Ref. [29]), could discriminate further between the 8 different right-handed neutrino mass spectra, and are worth studying in detail. We note in particular that the typical values of the mixing angles in  $U_m$  allowing solution  $(+, -, +)$  to be successful tend to enhance the branching ratios of processes like  $\mu \rightarrow e\gamma$  and  $\tau \rightarrow \mu\gamma$ .

Finally, it would be interesting to investigate how the results presented in this paper would be modified if the  $SU(2)_L$  doublet components of the  $\mathbf{126}$  were allowed to acquire a vev. In such a case, the mass relations  $M_d = M_e$  and  $M_D = M_u$  receive corrections proportional to the matrix  $f$ , and the measured down quark and charged lepton masses can be accounted for without introducing non-renormalizable interactions. However, a technical complication arises from the fact that the reconstruction procedure cannot be performed independently of the charged fermion mass fit. We defer the study of this case to future work.

<sup>17</sup>Although we only presented results for four reference solutions, we checked that the solutions that differ by  $x_1^+ \leftrightarrow x_1^-$ , such as  $(+, -, +)$  and  $(-, -, +)$ , show similar behaviour for  $Y_B$ .

## Acknowledgments

We thank M. Frigerio, T. Hambye and J.-M. Frère for useful comments, as well as T. Konstandin for discussions about Ref. [30]. This work has been supported in part by the projects ANR-05-BLAN-0193-02 and ANR-05-JCJC-0023 of the French Agence Nationale de la Recherche. PH and SL acknowledge partial support from the RTN European Program MRTN-CT-2004-503369. The research of PH was supported in part by the Marie Curie Excellence Grant MEXT-CT-2004-01429717.

## A Appendix: corrections to the mass relation $M_d = M_e$

In this appendix, we discuss the corrections to the GUT-scale mass relation  $M_d = M_e$  arising from non-renormalizable operators of the form:

$$\frac{\kappa_{ij}}{\Lambda} \mathbf{16}_i \mathbf{16}_j (\mathbf{10}_1 \times \mathbf{45})_{\mathbf{120}} , \quad (\text{A.1})$$

where only the  $Y = -1$   $SU(2)_L$  doublet in  $\mathbf{10}_1$  acquires a vev, so that the mass relation  $M_D = M_u$  is not affected, and the  $\mathbf{10}_1$  and  $\mathbf{45}$  Higgs representations are contracted in an effective  $\mathbf{120}$  representation, implying that the couplings  $\kappa_{ij}$  are antisymmetric. Such operators generate a contribution to the down quark and charged lepton masses when the  $\mathbf{45}$  acquires a vev in the  $T_{3R}$  or  $B - L$  direction. Indeed, the decomposition of the tensor product  $(\mathbf{10} \times \mathbf{45})_{\mathbf{120}}$  under the Pati-Salam subgroup  $SU(2)_L \times SU(2)_R \times SU(4)_c$  contains a  $(\mathbf{2}, \mathbf{2}, \mathbf{1})$  representation generated by  $(\mathbf{2}, \mathbf{2}, \mathbf{1})_{\mathbf{10}} \times (\mathbf{1}, \mathbf{3}, \mathbf{1})_{\mathbf{45}}$ , and a  $(\mathbf{2}, \mathbf{2}, \mathbf{15})$  representation generated by  $(\mathbf{2}, \mathbf{2}, \mathbf{1})_{\mathbf{10}} \times (\mathbf{1}, \mathbf{1}, \mathbf{15})_{\mathbf{45}}$ . The Clebsch-Gordan coefficients needed to distinguish  $M_d$  from  $M_e$  arise from  $(\mathbf{2}, \mathbf{2}, \mathbf{15})$ .

The most general situation occurs when the two vev's  $\langle (\mathbf{1}, \mathbf{3}, \mathbf{1}) \rangle$  in the  $T_{3R}$  direction and  $\langle (\mathbf{1}, \mathbf{1}, \mathbf{15}) \rangle$  in the  $B - L$  direction belong to different  $\mathbf{45}$ 's. We denote the scale of these vev's by  $v_3$  and  $v_{15}$  and assume that they have GUT scale values. The other dimensionful parameter appearing in Eq. (A.1) is  $\Lambda$ , which we identify with the scale at which the unified gauge coupling becomes non-perturbative,  $\Lambda \simeq 10 M_{GUT}$  [29]. The corrected mass matrices read:

$$M_d = M_d^{10} + \left( -\frac{v_3}{\Lambda} \kappa_1 + \frac{v_{15}}{\Lambda} \kappa_2 \right) v_d^{10_1} , \quad M_e = M_d^{10} + \left( -\frac{v_3}{\Lambda} \kappa_1 - 3 \frac{v_{15}}{\Lambda} \kappa_2 \right) v_d^{10_1} , \quad (\text{A.2})$$

where  $M_d^{10}$  is the contribution of the  $\mathbf{10}$ 's,  $v_d^{10_1}$  is the vev of the  $Y = -1$  Higgs doublet in  $\mathbf{10}_1$ , and the matrices  $\kappa_1$  and  $\kappa_2$  contain the non-renormalizable couplings associated with the two  $\mathbf{45}$ 's.

In order to study the corrected mass matrices, it is convenient to switch to the basis where the symmetric contribution  $M_d^{10}$  is diagonal. Then  $M_d$  and  $M_e$  can be parametrized as:

$$M_d = \begin{pmatrix} \mu_1 & \varepsilon_1 & \varepsilon_2 \\ -\varepsilon_1 & \mu_2 & \varepsilon_3 \\ -\varepsilon_2 & -\varepsilon_3 & \mu_3 \end{pmatrix} , \quad M_e = \begin{pmatrix} \mu_1 & -x_1 \varepsilon_1 & -x_2 \varepsilon_2 \\ x_1 \varepsilon_1 & \mu_2 & -x_3 \varepsilon_3 \\ x_2 \varepsilon_2 & x_3 \varepsilon_3 & \mu_3 \end{pmatrix} , \quad (\text{A.3})$$

with  $\mu_i$  real and  $\varepsilon_i$ ,  $x_i$  complex ( $\mu_i$  and  $\varepsilon_i$  are dimensionful parameters). This structure simplifies in some cases. If the vev's in the  $T_{3R}$  and  $B - L$  directions are carried by the same  $\mathbf{45}$ , there is a single matrix of non-renormalizable couplings  $\kappa$  and all  $x_i$  are equal. In the absence of a vev in the  $T_{3R}$  direction, one has  $x_1 = x_2 = x_3 = 3$ . The matrices  $M_d^\dagger M_d$  and  $M_e^\dagger M_e$  can easily be diagonalized in the case of hierarchical entries,  $\mu_1 \ll \mu_2 \ll \mu_3$  and  $|\varepsilon_1| \ll |\varepsilon_2| \ll |\varepsilon_3|$ , yielding:

$$m_b^2 \simeq \mu_3^2 + 2|\varepsilon_3|^2 , \quad (\text{A.4})$$

$$m_\tau^2 \simeq \mu_3^2 + 2|x_3 \varepsilon_3|^2 , \quad (\text{A.5})$$

$$m_b m_s \simeq |\mu_2 \mu_3 + \varepsilon_3^2| , \quad (\text{A.6})$$

$$m_\tau m_\mu \simeq |\mu_2 \mu_3 + x_3^2 \varepsilon_3^2| . \quad (\text{A.7})$$

The fact that  $\varepsilon_3^2$  appears in all four relations (A.4)–(A.7) implies that antisymmetric corrections can at most accommodate a GUT-scale  $\tau - b$  mass difference of the order of  $m_\mu$ , and this conclusion also holds for more general hierarchies of the  $\mu_i$  and  $\varepsilon_i$  parameters. This is not enough to account for the value of  $(m_\tau - m_b)$  obtained by running the measured down quark and charged lepton masses from  $M_Z$  to  $M_{GUT} = 2 \times 10^{16}$  GeV (assuming an effective supersymmetric threshold  $M_{SUSY} = 1$  TeV and  $\tan\beta = 10$ ):

$$\begin{aligned} m_d(M_{GUT}) &= 0.94 \text{ MeV} , & m_s(M_{GUT}) &= 17 \text{ MeV} , & m_b(M_{GUT}) &= 0.98 \text{ GeV} , \\ m_e(M_{GUT}) &= 0.346 \text{ MeV} , & m_\mu(M_{GUT}) &= 73.0 \text{ MeV} , & m_\tau(M_{GUT}) &= 1.25 \text{ GeV} . \end{aligned} \quad (\text{A.8})$$

However, we did not include in our analysis the low-energy supersymmetric threshold corrections to the bottom quark mass, which can substantially modify the value of  $m_b(M_{GUT})$  [78]. These corrections take the form:

$$m_b = (1 + \epsilon_b \tan\beta) y_b v_d , \quad (\text{A.9})$$

with the coefficient  $\epsilon_b$  given by:

$$\epsilon_b = \frac{2\alpha_3}{3\pi} \frac{\mu M_3}{m_{\tilde{b}_R}^2} f(M_3^2, m_{\tilde{b}_L}^2, m_{\tilde{b}_R}^2) + \frac{y_t^2}{16\pi^2} \frac{\mu A_t}{m_{\tilde{b}_R}^2} f(\mu^2, m_{\tilde{t}_L}^2, m_{\tilde{t}_R}^2) , \quad (\text{A.10})$$

where  $f$  is a loop function defined by:

$$f(m_1^2, m_2^2, m_3^2) = \left[ \frac{m_1^2}{m_3^2 - m_1^2} \ln\left(\frac{m_1^2}{m_3^2}\right) - \frac{m_2^2}{m_3^2 - m_2^2} \ln\left(\frac{m_2^2}{m_3^2}\right) \right] \frac{m_3^2}{m_1^2 - m_2^2} . \quad (\text{A.11})$$

The function  $f$  is of order one for superpartner masses between 100 GeV and 1 TeV, yielding typical values of  $\epsilon_b \sim 2\%$ . Due to the  $\tan\beta$  enhancement, the threshold corrections can thus reach the 20% level for  $\tan\beta = 10$ . This is enough to reach  $m_b(M_{GUT}) \simeq 1.17$  GeV, making it possible for the antisymmetric corrections to the GUT-scale mass relation  $M_d = M_e$  to account for the measured down quark and charged lepton masses.

Indeed, very good fits of the charged lepton and down quark masses can be obtained once supersymmetric threshold corrections are taken into account. Since the quality of the fit does not depend on the precise values of the  $x_i$ , we restrict ourselves to the case of a single **45** vev in the  $(\mathbf{1}, \mathbf{1}, \mathbf{15})$  direction, i.e. we set  $x_1 = x_2 = x_3 = \mathbf{3}$  in Eq. (A.3). For each set of parameters  $(\mu_i, \varepsilon_i)$  providing a good fit,  $M_d$  and  $M_e$  are determined as well as the mismatch matrix  $U_m$  introduced in Section 4.2. Since only  $U_m$  is needed for the computation of the final baryon asymmetry, we concentrate on this matrix from now on. Let us introduce the following parametrization:

$$U_m = e^{i\phi_g^m} \begin{pmatrix} e^{i\phi_1^m} & 0 & 0 \\ 0 & e^{i\phi_2^m} & 0 \\ 0 & 0 & 1 \end{pmatrix} V(\theta_{12}^m, \theta_{13}^m, \theta_{23}^m, \delta^m) \begin{pmatrix} e^{i\phi_3^m} & 0 & 0 \\ 0 & e^{i\phi_4^m} & 0 \\ 0 & 0 & 1 \end{pmatrix} , \quad (\text{A.12})$$

where  $V$  is a CKM-like matrix with three real angles and a complex phase. As Eq. (A.3) contains more parameters than needed to fit the down-type fermion masses, we fix some of them, such as  $|\varepsilon_1|$  and the phase of  $\varepsilon_2$ . For  $|\varepsilon_1| \ll |\varepsilon_2|$ , which roughly corresponds to  $|\varepsilon_1| \lesssim 0.001$  GeV, good fits generally correspond to values of the  $\theta_{ij}^m$ 's of the order of the Cabibbo angle or smaller, for instance:

$$\theta_{12}^m \approx 0.3 , \quad \theta_{13}^m \approx 0.1 , \quad \theta_{23}^m \approx 0.35 . \quad (\text{A.13})$$

For larger values of  $|\varepsilon_1|$  ( $|\varepsilon_1| \gtrsim 0.001$  GeV), one can obtain larger (1, 2) and (1, 3) mixing angles, e.g.:

$$\theta_{12}^m \approx 1 , \quad \theta_{13}^m \approx 0.2 , \quad \theta_{23}^m \approx 0.2 . \quad (\text{A.14})$$

In our numerical study of leptogenesis, we use different choices for  $U_m$ , combined with a non-vanishing high-energy or Majorana phase that we fix at  $\pi/4$ . The resulting four sets of parameters are displayed in the table below:

set	$\theta_{12}^m$	$\theta_{13}^m$	$\theta_{23}$	$\delta^m$	$\phi_g^m$	$\phi_1^m$	$\phi_2^m$	$\phi_3^m$	$\phi_4^m$	$\pi/4$
1	1.07	0.22	0.21	5.80	3.21	4.37	5.86	0.87	6.16	$\Phi_2^u$
2	1.07	0.22	0.21	5.80	3.21	4.37	5.86	0.87	6.16	$\Phi_2^v$
3	0.28	0.089	0.37	0.062	3.15	3.12	6.03	2.94	6.19	$\Phi_2^u$
4	0.17	0.066	0.29	0.23	3.14	0.54	0.015	6.27	0.0032	$\Phi_2^u$

To illustrate the influence of  $U_m$  on the leptogenesis parameters, we plot in Fig. 11 the CP asymmetry  $\epsilon_{1\tau}$  and the washout parameter  $\tilde{m}_{1\mu}$  for different values of  $\theta_{12}^m$ . Part of the effect which can be seen is due to the influence of the  $\theta_{ij}^m$ 's on the right-handed neutrino masses.

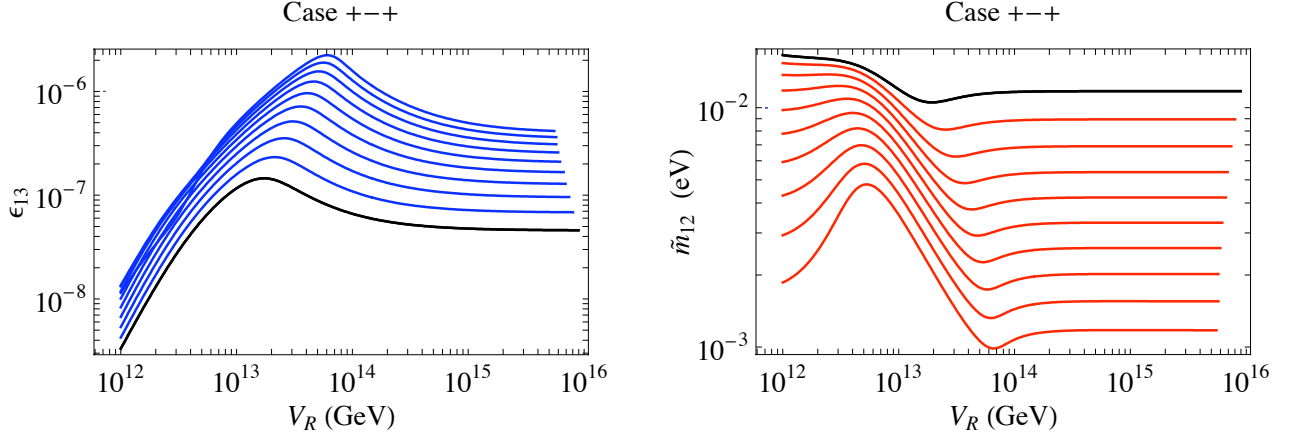


Figure 11:  $\epsilon_{1\tau}$  and  $\tilde{m}_{1\mu}$  as a function of  $v_R$  in the  $(+, -, +)$  solution, for  $\Phi_2^u = \pi/4$  and different values of  $\theta_{12}^m \in [0, \pi/4]$ . All other parameters in  $U_m$  and high-energy phases are set to zero. The reference case  $\theta_{12}^m = 0$  ( $U_m = \mathbf{1}$ ) is plotted in black. The other input parameters are as in Fig. 2.

## References

- [1] D. N. Spergel *et al.* [WMAP Collaboration], *Astrophys. J. Suppl.* **170** (2007) 377 [arXiv:astro-ph/0603449]; G. Hinshaw *et al.* [WMAP Collaboration], arXiv:0803.0732 [astro-ph].
- [2] M. Fukugita and T. Yanagida, *Phys. Lett. B* **174** (1986) 45.
- [3] N. S. Manton, *Phys. Rev. D* **28** (1983) 2019; F. R. Klinkhamer and N. S. Manton, *Phys. Rev. D* **30** (1984) 2212.
- [4] S. Y. Khlebnikov and M. E. Shaposhnikov, *Nucl. Phys. B* **308** (1988) 885; J. A. Harvey and M. S. Turner, *Phys. Rev. D* **42** (1990) 3344.
- [5] For a recent review and a list of references, see S. Davidson, E. Nardi and Y. Nir, arXiv:0802.2962 [hep-ph].
- [6] S. Davidson and A. Ibarra, *Phys. Lett. B* **535** (2002) 25 [arXiv:hep-ph/0202239].
- [7] W. Buchmuller, P. Di Bari and M. Plumacher, *Nucl. Phys. B* **643** (2002) 367 [Erratum-ibid. B **793** (2008) 362] [arXiv:hep-ph/0205349].
- [8] G. F. Giudice, A. Notari, M. Raidal, A. Riotto and A. Strumia, *Nucl. Phys. B* **685** (2004) 89 [arXiv:hep-ph/0310123].
- [9] W. Buchmuller and M. Plumacher, *Phys. Lett. B* **511** (2001) 74 [arXiv:hep-ph/0104189].

- [10] R. Barbieri, P. Creminelli, A. Strumia and N. Tetradis, Nucl. Phys. B **575** (2000) 61 [arXiv:hep-ph/9911315].
- [11] P. Minkowski, Phys. Lett. B **67** (1977) 421; M. Gell-Mann, P. Ramond and R. Slansky, in *Supergravity*, P. van Nieuwenhuizen and D.Z. Freedman (eds.), North Holland Publ. Co., 1979, p. 315; T. Yanagida, in *Proc. of the Workshop on the Baryon Number of the Universe and Unified Theories*, O. Sawada and A. Sugamoto (eds.), Tsukuba, Japan, 13-14 Feb. 1979, p. 95; S. L. Glashow, in *Quarks and Leptons*, Cargèse Lectures, 9-29 July 1979, Plenum, New York, 1980, p. 687; R. N. Mohapatra and G. Senjanovic, Phys. Rev. Lett. **44** (1980) 912.
- [12] V. A. Kuzmin, V. A. Rubakov and M. E. Shaposhnikov, Phys. Lett. B **155** (1985) 36.
- [13] M. B. Gavela, P. Hernandez, J. Orloff, O. Pene and C. Quimbay, Nucl. Phys. B **430** (1994) 382 [arXiv:hep-ph/9406289].
- [14] K. Kajantie, M. Laine, K. Rummukainen and M. E. Shaposhnikov, Phys. Rev. Lett. **77** (1996) 2887 [arXiv:hep-ph/9605288].
- [15] M. S. Carena, M. Quiros and C. E. M. Wagner, Phys. Lett. B **380** (1996) 81 [arXiv:hep-ph/9603420]; D. Delepine, J. M. Gerard, R. Gonzalez Felipe and J. Weyers, Phys. Lett. B **386** (1996) 183 [arXiv:hep-ph/9604440].
- [16] J. M. Cline, arXiv:hep-ph/0609145.
- [17] H. Georgi, AIP Conf. Proc. **23** (1975) 575; H. Fritzsch and P. Minkowski, Annals Phys. **93** (1975) 193.
- [18] E. Nezri and J. Orloff, JHEP **0304** (2003) 020 [arXiv:hep-ph/0004227]; G. C. Branco, R. Gonzalez Felipe, F. R. Joaquim and M. N. Rebelo, Nucl. Phys. B **640** (2002) 202 [arXiv:hep-ph/0202030].
- [19] E. K. Akhmedov, M. Frigerio and A. Y. Smirnov, JHEP **0309** (2003) 021 [arXiv:hep-ph/0305322].
- [20] C. S. Aulakh, B. Bajc, A. Melfo, G. Senjanovic and F. Vissani, Phys. Lett. B **588** (2004) 196 [arXiv:hep-ph/0306242]. For a brief discussion of leptogenesis in this model, see T. Fukuyama, arXiv:0806.1987 [hep-ph].
- [21] J. C. Pati, Phys. Rev. D **68** (2003) 072002; C. H. Albright and S. M. Barr, Phys. Rev. D **70** (2004) 033013 [arXiv:hep-ph/0404095]; X. d. Ji, Y. c. Li, R. N. Mohapatra, S. Nasri and Y. Zhang, Phys. Lett. B **651** (2007) 195 [arXiv:hep-ph/0605088]; T. Kikuchi, arXiv:0802.3470 [hep-ph].
- [22] P. Di Bari, Nucl. Phys. B **727** (2005) 318 [arXiv:hep-ph/0502082].
- [23] O. Vives, Phys. Rev. D **73** (2006) 073006 [arXiv:hep-ph/0512160].
- [24] T. Asaka, Phys. Lett. B **562** (2003) 291 [arXiv:hep-ph/0304124].
- [25] M. Frigerio, P. Hosteins, S. Lavignac and A. Romanino, arXiv:0804.0801 [hep-ph].
- [26] J. C. Romao, M. A. Tortola, M. Hirsch and J. W. F. Valle, Phys. Rev. D **77** (2008) 055002 [arXiv:0707.2942 [hep-ph]]; S. K. Majee, M. K. Parida and A. Raychaudhuri, arXiv:0807.3959 [hep-ph].
- [27] M. Magg and C. Wetterich, Phys. Lett. B **94** (1980) 61; G. Lazarides, Q. Shafi and C. Wetterich, Nucl. Phys. B **181** (1981) 287; R. N. Mohapatra and G. Senjanovic, Phys. Rev. D **23** (1981) 165.
- [28] E. K. Akhmedov and M. Frigerio, Phys. Rev. Lett. **96** (2006) 061802 [arXiv:hep-ph/0509299].
- [29] P. Hosteins, S. Lavignac and C. A. Savoy, Nucl. Phys. B **755** (2006) 137 [arXiv:hep-ph/0606078].

- [30] E. K. Akhmedov, M. Blennow, T. Hallgren, T. Konstandin and T. Ohlsson, JHEP **0704** (2007) 022 [arXiv:hep-ph/0612194].
- [31] T. Hallgren, T. Konstandin and T. Ohlsson, JCAP **0801** (2008) 014 [arXiv:0710.2408 [hep-ph]].
- [32] H. S. Goh, R. N. Mohapatra and S. Nasri, Phys. Rev. D **70** (2004) 075022 [arXiv:hep-ph/0408139].
- [33] K. S. Babu and R. N. Mohapatra, Phys. Rev. Lett. **70** (1993) 2845 [arXiv:hep-ph/9209215].
- [34] M. Jamin, “Quark masses”, talk given at the University of Granada, March 2006 (<http://personal.ifaef.es/jamin/my/talks/mq-granada06.pdf>).
- [35] W. M. Yao *et al.* [Particle Data Group], J. Phys. G **33** (2006) 1.
- [36] S. Antusch, J. Kersten, M. Lindner, M. Ratz and M. A. Schmidt, JHEP **0503** (2005) 024 [arXiv:hep-ph/0501272]; <http://users.physik.tu-muenchen.de/rge/REAP/index.html>.
- [37] G. L. Fogli, E. Lisi, A. Marrone and A. Palazzo, Prog. Part. Nucl. Phys. **57** (2006) 742 [arXiv:hep-ph/0506083].
- [38] M. Y. Khlopov and A. D. Linde, Phys. Lett. B **138** (1984) 265; J. R. Ellis, J. E. Kim and D. V. Nanopoulos, Phys. Lett. B **145** (1984) 181.
- [39] M. Bolz, A. Brandenburg and W. Buchmuller, Nucl. Phys. B **606** (2001) 518 [Erratum-ibid. B **790** (2008) 336] [arXiv:hep-ph/0012052]; J. Pradler and F. D. Steffen, Phys. Rev. D **75** (2007) 023509 [arXiv:hep-ph/0608344]; V. S. Rychkov and A. Strumia, Phys. Rev. D **75** (2007) 075011 [arXiv:hep-ph/0701104].
- [40] T. Endoh, T. Morozumi and Z. h. Xiong, Prog. Theor. Phys. **111** (2004) 123 [arXiv:hep-ph/0308276].
- [41] A. Abada, S. Davidson, F. X. Josse-Michaux, M. Losada and A. Riotto, JCAP **0604** (2006) 004 [arXiv:hep-ph/0601083].
- [42] E. Nardi, Y. Nir, E. Roulet and J. Racker, JHEP **0601** (2006) 164 [arXiv:hep-ph/0601084].
- [43] A. Abada, S. Davidson, A. Ibarra, F. X. Josse-Michaux, M. Losada and A. Riotto, JHEP **0609** (2006) 010 [arXiv:hep-ph/0605281].
- [44] S. Blanchet and P. Di Bari, JCAP **0703** (2007) 018 [arXiv:hep-ph/0607330].
- [45] S. Antusch, S. F. King and A. Riotto, JCAP **0611** (2006) 011 [arXiv:hep-ph/0609038].
- [46] S. Pascoli, S. T. Petcov and A. Riotto, Phys. Rev. D **75** (2007) 083511 [arXiv:hep-ph/0609125], Nucl. Phys. B **774** (2007) 1 [arXiv:hep-ph/0611338].
- [47] G. C. Branco, R. Gonzalez Felipe and F. R. Joaquim, Phys. Lett. B **645** (2007) 432 [arXiv:hep-ph/0609297].
- [48] S. Antusch and A. M. Teixeira, JCAP **0702** (2007) 024 [arXiv:hep-ph/0611232].
- [49] S. Blanchet, P. Di Bari and G. G. Raffelt, JCAP **0703** (2007) 012 [arXiv:hep-ph/0611337].
- [50] A. De Simone and A. Riotto, JCAP **0702** (2007) 005 [arXiv:hep-ph/0611357].
- [51] F. X. Josse-Michaux and A. Abada, JCAP **0710** (2007) 009 [arXiv:hep-ph/0703084].
- [52] T. Shindou and T. Yamashita, JHEP **0709** (2007) 043 [arXiv:hep-ph/0703183].

- [53] S. Antusch, Phys. Rev. D **76** (2007) 023512 [arXiv:0704.1591 [hep-ph]].
- [54] S. Blanchet and P. Di Bari, JCAP **0606** (2006) 023 [arXiv:hep-ph/0603107].
- [55] G. Engelhard, Y. Grossman, E. Nardi and Y. Nir, Phys. Rev. Lett. **99** (2007) 081802 [arXiv:hep-ph/0612187].
- [56] L. Covi, E. Roulet and F. Vissani, Phys. Lett. B **384** (1996) 169 [arXiv:hep-ph/9605319].
- [57] T. Hambye and G. Senjanovic, Phys. Lett. B **582** (2004) 73 [arXiv:hep-ph/0307237].
- [58] S. Antusch and S. F. King, Phys. Lett. B **597** (2004) 199 [arXiv:hep-ph/0405093].
- [59] A. Pilaftsis and T. E. J. Underwood, Nucl. Phys. B **692** (2004) 303 [arXiv:hep-ph/0309342]; A. Pilaftsis, Phys. Rev. Lett. **95** (2005) 081602 [arXiv:hep-ph/0408103]; A. Pilaftsis and T. E. J. Underwood, Phys. Rev. D **72** (2005) 113001 [arXiv:hep-ph/0506107].
- [60] W. Buchmuller, P. Di Bari and M. Plumacher, Annals Phys. **315** (2005) 305 [arXiv:hep-ph/0401240].
- [61] M. Plumacher, Nucl. Phys. B **530** (1998) 207 [arXiv:hep-ph/9704231].
- [62] E. Nardi, J. Racker and E. Roulet, JHEP **0709** (2007) 090 [arXiv:0707.0378 [hep-ph]].
- [63] E. Ma, S. Sarkar and U. Sarkar, Phys. Lett. B **458** (1999) 73 [arXiv:hep-ph/9812276].
- [64] S. Carlier, J. M. Frere and F. S. Ling, Phys. Rev. D **60** (1999) 096003 [arXiv:hep-ph/9903300].
- [65] N. Cosme, JHEP **0408** (2004) 027 [arXiv:hep-ph/0403209].
- [66] D. J. H. Chung, B. Garbrecht and S. Tulin, arXiv:0807.2283 [hep-ph].
- [67] M. Kawasaki, K. Kohri, T. Moroi and A. Yotsuyanagi, arXiv:0804.3745 [hep-ph].
- [68] F. Hahn-Woernle and M. Plumacher, arXiv:0801.3972 [hep-ph].
- [69] G. Anderson, S. Raby, S. Dimopoulos, L. J. Hall and G. D. Starkman, Phys. Rev. D **49** (1994) 3660 [arXiv:hep-ph/9308333].
- [70] T. Schwetz, AIP Conf. Proc. **981** (2008) 8 [arXiv:0710.5027 [hep-ph]].
- [71] C. S. Aulakh, B. Bajc, A. Melfo, A. Rasin and G. Senjanovic, Nucl. Phys. B **597** (2001) 89 [arXiv:hep-ph/0004031].
- [72] T. Kanzaki, M. Kawasaki, K. Kohri and T. Moroi, Phys. Rev. D **75** (2007) 025011 [arXiv:hep-ph/0609246].
- [73] W. Buchmuller, L. Covi, K. Hamaguchi, A. Ibarra and T. Yanagida, JHEP **0703** (2007) 037 [arXiv:hep-ph/0702184].
- [74] H. Pagels and J. R. Primack, Phys. Rev. Lett. **48** (1982) 223.
- [75] M. Viel, J. Lesgourgues, M. G. Haehnelt, S. Matarrese and A. Riotto, Phys. Rev. D **71** (2005) 063534 [arXiv:astro-ph/0501562].
- [76] S. Weinberg, Phys. Rev. Lett. **48**, 1303 (1982).
- [77] T. Gherghetta, G. F. Giudice and J. D. Wells, Nucl. Phys. B **559** (1999) 27 [arXiv:hep-ph/9904378].
- [78] K. S. Babu and C. F. Kolda, Phys. Lett. B **451** (1999) 77 [arXiv:hep-ph/9811308]; K. Tobe and J. D. Wells, Nucl. Phys. B **663** (2003) 123 [arXiv:hep-ph/0301015]; G. Ross and M. Serna, arXiv:0704.1248 [hep-ph].